RICE UNIVERSITY

Protease-Activated Quantum Dot Probes

by

Nima Rohani

A THESIS SUBMITTED
IN PARTIAL FULFILLMENT OF THE
REQUIREMENTS FOR THE DEGREE

Master of Science

APPROVED, THESIS COMMITTEE

Jennifer L. West, Chair, Isabel C. Cameron Professor, Bioengineering

Rebekah Drezek, Associate Professor, Bioengineering

Vicki L. Colvin, Kenneth S. Pitzer-Schlumberger Professor, Chemistry

HOUSTON, TEXAS
JANUARY 2011

Abstract

Protease-Activated Quantum Dot Probes

by

Nima Rohani

Protease activity has been demonstrated to be an important prognostic and predictive marker in diseases such as cancer and stroke. As such, much attention has been given to the development of diagnostic tools that would allow one to assay their activity in living tissues. Protease activity is regulated at many levels including transcription, translation, activation, and inhibition and in order to derive the maximum prognostic benefit, it is essential to study their activity within this complex environment. Initial attempts to accomplish this goal involved the use of organic fluorophores pairs that utilize Fluorescence Resonance Energy Transfer (FRET) but suffered many drawbacks. Quantum Dots (QD) have addressed many of the drawbacks of organic fluorophores in various optical imaging applications. These include a decreased sensitivity to photobleaching and chemical degradation, size-tunable narrow emission peaks, and broad absorbance allowing excitation of multiple peak emission QD by one excitation source. In this work, we propose to utilize Quantum Dots (QD) linked to gold nanoparticles (AuNPs) by protease cleavable peptide sequences to serve as probes for assaying protease activity both *in vivo* and *in vitro*. This work involved the synthesis and characterization of the various components necessary for the probe design as well as the optimization of probe characteristics to achieve highly biocompatible probes that exhibit both a high level of quenching and maximum fluorescence recovery in the presence of protease. Probe functionality was optimized and it was determined that probes with AuNP:QD ratio of 10:1 and peptide linker length of 6.5 nm resulted in highest and most linear fluorescent signal gain. The ability to multiplex probes was also validated by developing spectrally orthogonal probes sensitive to collagenase and cathepsin K. Our design is expected to have many applications in the research and understanding of the role of proteases in disease and as a predictive tool for the prognosis of diseases such as cancer.

Acknowledgements

First and foremost I would like to thank Dr. Jennifer West, Dr. Rebekah Drezek, and Dr. Vicki Colvin for graciously accepting to be on my committee. I would also like to thank the members of the West lab for their help and support and for creating an environment that was both educational and supportive. I would also like to thank Nastassja Lewinski for her assistance in getting started with quantum dots and Huigang Zhu for his assistance in development of water solubilized quantum dots that were crucial to the project. Finally, I would like to thank my family for their love and support throughout the course of my project. If it were not for the love and encouragement provided by my parents as well as my sister, I do not think I would have been able to complete this project.

Table of Contents

List of Figures

Chapter 1: Introduction

1.1. Enhanced Diagnostics

1.1.1. Introduction

In recent times, advances in many fields of biological research has opened the door for innovative treatments of various diseases. In addition, these same advances have allowed us to adopt a more systematic approach to medicine. Rather than having to wait for symptom onset and proceeding to generic treatment, personalized medicine aims to use these advances to tackle disease detection, screening, diagnosis, prognosis, and prediction on a more individualized basis. These various intervention points can be seen in Figure 1.

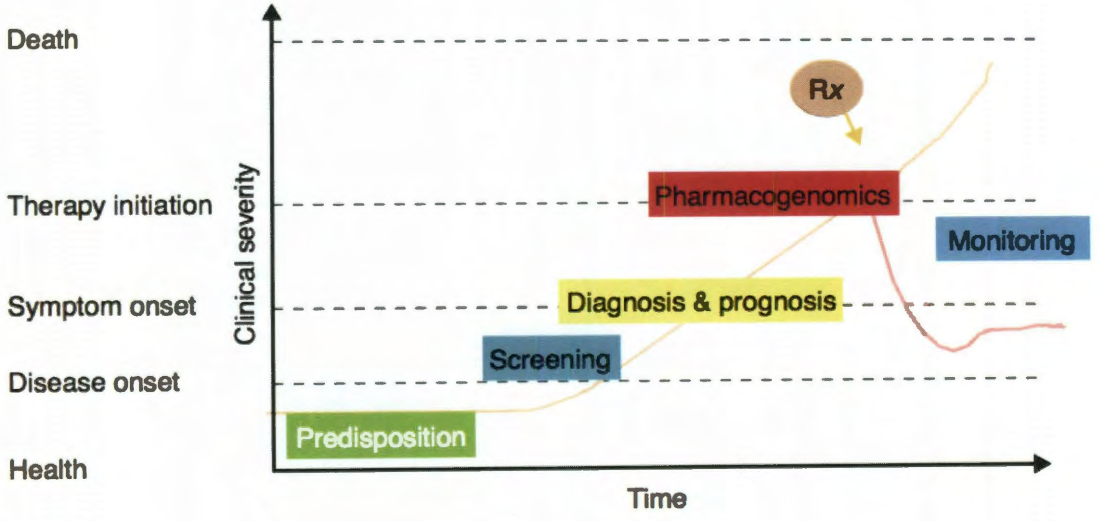

Figure 1 - Points of Intervention for Personalized Medicine

From Myer et al. 2002[1]

In many diseases, such as cancer, where the choice of treatment and variation in disease characteristics varies greatly from person to person, there is an especially important need to develop predictive markers for patient response to treatment. This need for predictive markers is highlighted by the fact that there are 2.2 million hospitalizations and over 100,000 deaths a year due to harmful drug reactions and side-effects[2]. The ability to personalize treatment on the basis of an individual's specific disease state would greatly help reduce this number.

This is especially vital to cancer as the therapeutic choices, which have become more aggressive over the last 20 years[3], are linked to quite undesirable side effects[4,5]. Furthermore, many new therapies, such as imatinib, gefitinib, and cetuximab are effective only in cases where specific molecular markers are expressed at sufficient levels[6]. While work is being undertaken to develop diagnostic tools for all stages of cancer care, much attention is being given to the need to develop prognostic and predictive markers to guide treatment. An example of such markers is the family of cysteine cathepsins and their endogenous inhibitors. It has been shown that the activity of cysteine cathepsins is up-regulated in invasive cancers due to a disruption balance between cathepsins and their inhibitors. Thus, cathepsin activity has been shown to be a good marker for survival length, relapse risk, and mortality and as such their ability to guide cancer therapy has been studied[7]. Also of note are estreogen receptor (ER) and a surface-bound receptor tyrosine kinase (Her2/Neu,), presence which guide the use of tamoxifen and trastuzumab[6].

This need for prognostic and predictive markers ranges well beyond cancer. In Rheumatoid arthritis, where an increasing number of therapeutic choices have become

available, methodologies for predicting patient response have become more and more crucial. This is heightened by the high cost and the known side-effects of the various treatments[8]. Finally, the field of pharmacology is in dire need of markers for determining the pharmacokinetic, pharmacodynamic, and idiosyncratic response to various drugs[9]. As one example of this need, a recent study has shown that various factors can easily result in 600-fold differences in drug plasma concentrations in individuals of the same weight on the same dosage[10]. This is particularly important in the area of. cancer research, where proteolytic activity can highly affect drug distribution.

1.1.2. Important Markers for Disease Diagnosis

Having seen the need for prognostic and predictive indicators in disease, attention must be given to identifying such markers. Initial research in this field began as the understanding that genetic variability was linked to disease response and progression[11]. In 1959, before the development of the modern genetics era, the field of pharmaco-genetics had already been proposed[12]. The completion of the Human Genome project in 2003[13], helped propel the field of genomics even further. Since then, work to identify biomarkers has expanded from the realm of genomics to include proteomics and degradomics.

Efforts in the area of genomics have focused mainly on Single-Nucleotide Polymorphisms[14], gene-expression patterns[15], oncoviral markers[16], and mutations in mitochondrial DNA[17]. Similar efforts in the field of proteomics are working towards the development of proteomic profiles and markers for use in guiding therapy[18,19,20]. Particularly important to our proposed work is the area of degradomics or study of

proteases, their inhibitors, and substrates. This area, which in recent years has received more and more attention, uses the activity of proteases as markers for determining disease severity and allowing better prognostic and predictive diagnosis for patients. Many such proteases have been identified including urokinase plasminogen activator, cathepsins B, D, and L, as well as various matrix metallo-proteases[21,22].

1.2. Proteases

1.2.1. Background

Proteases represent one set of markers that provide great promise as prognostic indicators of disease progress in cancer and other pathologies. As such, the proposed work focuses on providing a methodology for assaying their activity in living tissues. Proteases are a class of enzymes that result in the hydrolysis of peptide bonds in both proteins and polypeptides. Initially discovered as gastric enzymes involved in degradation of dietary proteins, they have since been defined as playing a key role in various cellular and biological functions[23]. These include but our not limited to bone formation, homeostatic tissue remodeling, cell signaling and migration, wound healing, angiogenesis, apoptosis, digestion, cellular proliferation and differentiation, and fertilization[23,24,]. Currently, 460 different proteases have been identified as part of the human genome with an additional 93 inactive homologue which are thought to be involved in protease regulation/inhibition[25]. These numerous proteases belong to five main families: aspartic, metallo, cysteine, serine and threonine proteases. Figure 2 shows the distribution of the human proteases and their cellular localization.

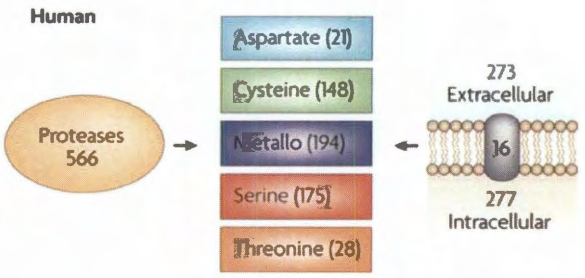

Figure 2 - Protease Families and Cellular Distribution

Modified from Overall et al. 2007[26]

These families use either covalent or acid-base catalysis to perform their hydrolytic function. The specificity of a given protease is defined by what sequences of peptides can be recognized by its active site. Figure 3 demonstrates the two forms of catalysis used by proteases and their binding to specific peptide sequences.

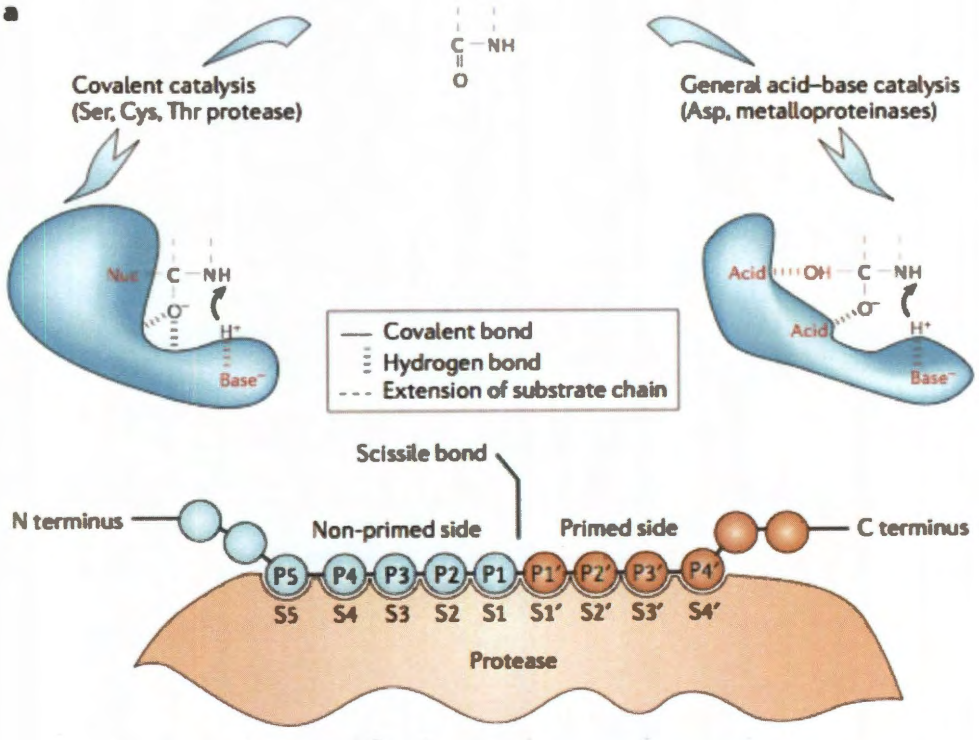

Figure 3 – Protease Hydrolytic Mechanism and Binding.

Modified from Turk et al. 2006[52]

While some of these proteases have specifically defined functions, most are involved in intricate webs or cascades of cellular events. This intricate balance of proteolytic activity is maintained by protease specificity, the presence of inhibitors, presence of peptide substrate, and protease activation. As they function to cleave bonds in various proteins and enzymes, they are involved in regulating many biological processes both intracellularly and in the extra-cellular matrix (ECM). Serving such a crucial role in so many biological functions, it is evident to see how any disruption of their function can lead to and be a marker for various pathologies.

1.2.2. Role of Proteases in Disease Progression

Proteases play an important role in many pathologies. In some of these diseases, the level of proteolytic activity can serve as a marker for specific disease state and progression, while in others an understanding of the role of proteases can help guide the development of treatment options.

Cancer, being a disease with such varied genetic causes, is one that would benefit greatly from the diagnostic insight that could be gained from protease activity. While all five families of proteases have been shown to play important roles in cancer development and progression, much of the research in relation to cancer has focused on one family of proteases, matrix-metallo proteases (MMPs). The up-regulation of MMPs in various forms of cancer is usually associated with poor prognosis[27]. Initial research into the role of proteases in cancer focused on their ability to degrade the ECM and thus facilitate both tumor growth and metastasis[28]. Since then, proteases have been increasingly implicated in all six hallmarks of cancer as defined by Hanahan et al[29].: self-support in growth

signals, insensitivity to growth-inhibitory signals, escape from apoptosis, infinite replication, sustained angiogenesis, and tissue invasion and metastasis[29]. A summary of the roles of MMPs in these 6 hallmarks is given in Figure 4.

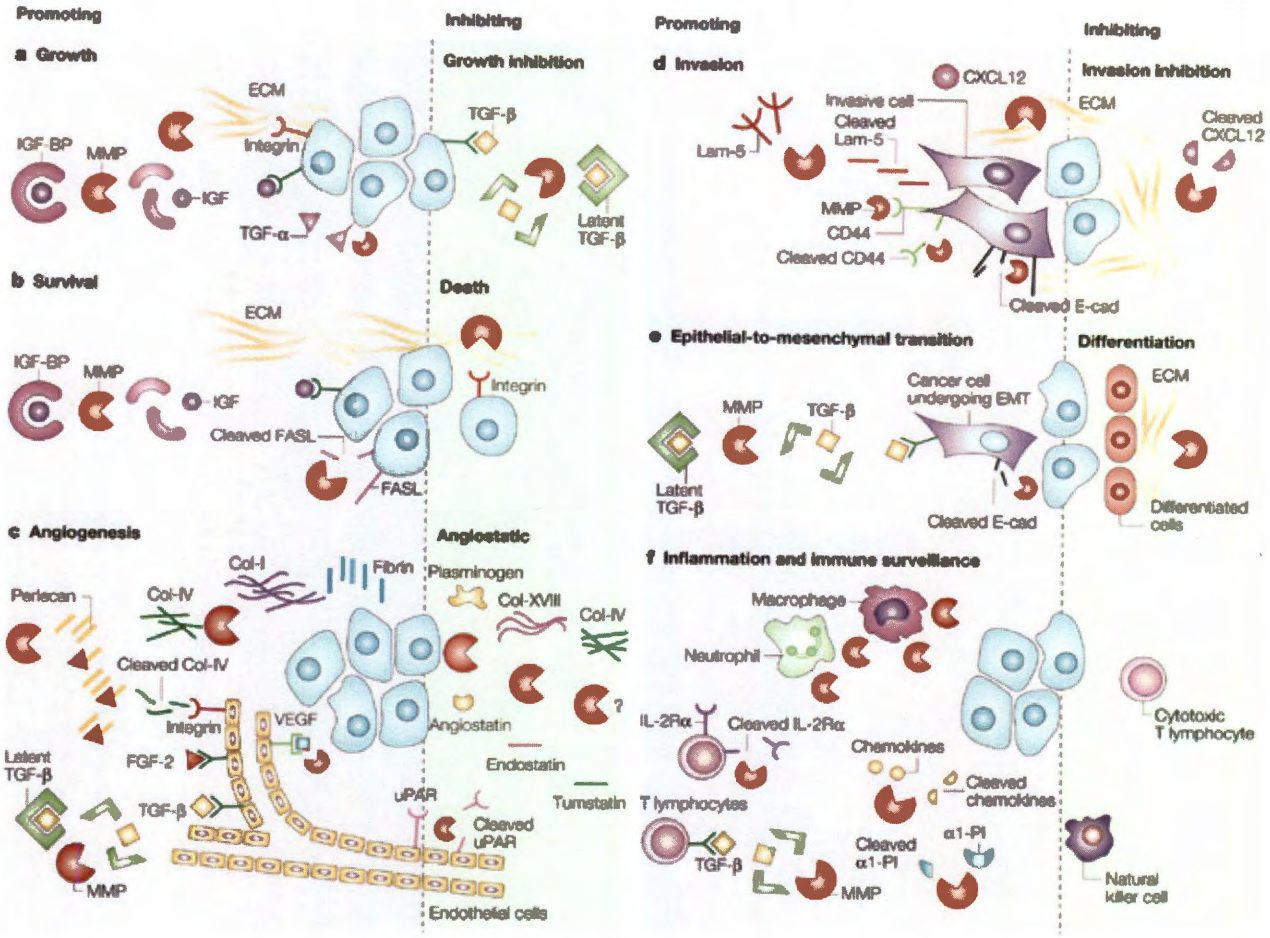

Figure 4 - Role of Proteases in 6 Hallmarks of Cancer

From Egelbad et al.[30]

The involvement of proteases, and MMPs in particular, in cancer cell growth is realized primarily by their ability to alter the availability of growth factors by releasing both membrane-bound growth factors[31] and the sequestered growth factors that are bound

to ECM components[32]. In addition, alterations of ECM components by increased MMP activity has been shown to affect ECM-cell signaling[33]. Proteases are also involved in allowing cancer cells to evade apoptosis through the down-regulation of apoptotic inhibitors such as MMP-3 and Caspase-1[34]. Proteases are further involved in cancer progression by inhibiting the body's immune response. This is accomplished by their ability to inhibit T-cell proliferation[35], activating TGF-β which inhibit T-lymphocytes[36], and increasing cancer-cell resistance to the immune system[37].

Angiogenesis, another crucial component of cancer development, is enabled by the increased activity of many proteases. Over-expression of MMP-2, which acts to cleave collagen type IV, leads to the exposure of a αvβ3 integrin-binding site and promotes tumor growth and angiogenesis[38]. MMP-9, which also has heightened activity in many cancers, plays a crucial role by leading to an increase in VEGF[39]. Finally, MMP-14 degrades the pericellular fibrin matrix surrounding vessels and allows endothelial invasion and outgrowth[40].

Finally, and most relevant to our proposed work, is the role of proteases in degrading ECM and thus promoting tumor invasion and metastasis. Three main systems of proteases have been heavily researched for their involvement in tumor metastasis, the serine protease urokinase-type plasminogen activator (uPA), the cysteine proteases such as cathepisn B, and MMPs. uPA has been showed to directly affect a cancer cells potential for invasion[41]. Many of the cathepsins have been shown to mark the transition to tumor invasiveness and malignancy and have been shown to be an indicator of metastatic potential[42]. The role of MMPs has also been greatly studied. These protease enable metastasis by activating cell-migration signals[43], promoting cell detachment from

the ECM by cleaving CD44[44] and E-cadherin[45], and enabling intravasation of cancer cells into the blood stream[46].

In addition to the roles proteases play in disease progression, it is important to understand how their expression and activity is regulated. Although cancer cells themselves are responsible for the increase in activity of certain proteases, their influence on protease secretion of stromal cells is equally if not more important. The mechanism by which cancer cells alter the expressions in their surrounding stromal cells is thought to involve secretion of interleukins, interferons, emmprin and growth factors[47]. This is important to keep in mind when developing *in vitro* models of cancer protease activity. To conclude, as proteases play such a crucial role in cancer progression and have been linked to tumor aggressiveness and to the likelihood of recurrence, protease activity can provide an important marker in the determination of optimal patient treatment.

In addition to cancer, proteases play a great role in various other diseases. In Multiple Sclerosis, proteases are involved in many of the stages defining the disease including demyelination, apoptosis, axon injury, and various elements of the inflammatory response involved[48]. Protease activity can thus be used as a target for developing treatments as well as being able to identify various stages of the disease progression.

In HIV, proteases play a big role in the spread of the virus by driving ECM degradation and allowing for the spread of the virus and granting it access to immuno-privileged locations in the body[49]. Proteases also play a role in many respiratory pathologies including allergies in which they play a great role in activating PAR-2

receptors[50]. Finally, a great deal of genetic disease exist that are as a result of over-activation or a deficiency in protease activity. 42 such disorders have currently been identified[51] which result in a variety of symptoms spanning over all major organs in the body. This wide range of disorders further goes to show the diversity of roles that proteases play in homeostasis.

1.2.3. Protease Regulation and Activation

The regulation of protease activity is a complex process involving protease production, activation, and inhibition. Proteases are generally produced as zymogen precursors in inactive form. The first level of cellular control is variation in transcription of the mRNA encoding these precursors and their translation into these inactive zymogens. Once present, the activation of these precursors presents the second level of regulation. This activation commonly occurs through the cleavage of C-terminal pro-peptides[52]. This activation occurs through one of three mechanisms: autocatalysis, activation by other proteases, or through the mechanism of an activation complex.

Having been activated, proteolytic activity is further regulated by the presence of inhibitors and cofactors. Inhibitors, which have been classified into 18 main families, operate by competing for and binding to the active sites of proteases[25]. These inhibitors are themselves regulated by the presence of co-factors which can reversibly bind and affect their function. Figure 5 demonstrates a simple view of protease regulation post-translation.

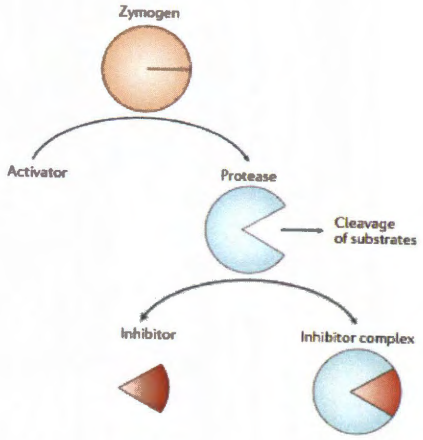

Figure 5 - Regulation of Protease Activity Post-Translation

From Turk et al. 2006[52]

The complex homeostatic balance created by these various control mechanisms produces a challenge to many genomic and proteomic approaches used to diagnose pathologies. While the regulation of protease levels plays a role in disease states, it is the over or under-regulation of proteolytic activity that is the greatest concern. As such, methodologies are required that can accurately assay such activity.

1.2.4. Protease Kinetics

The study of protease activity can be done in two fashions. The first is to try to profile the function of individual proteases[52]. The second is to study the cleavage of substrate particles. In both cases, an understanding of the kinetics involved is essential to the quantification and modeling of observed results.

The model commonly used to describe protease cleavage of peptide substrates is that of Michaelis-Menten kinetics[53,54,55,56]. The Michaelis-Menten model, initially proposed by Leonor Michaelis and Maud Menten in 1913[57], describes the rate at which

an enzyme with an excess of substrate catalyzes the product in question. The reaction being described can be seen below:

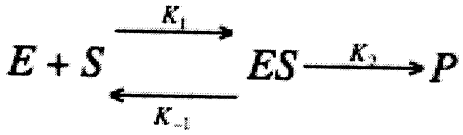

In this model, E describes the enzyme (protease) concentration, S denotes the substrate (peptide to be cleaved), and P denotes the products (cleaved peptides). Analysis of this model leads to the following equation[58] that describes the velocity of the reaction:

$$V = \frac{V_{max} \cdot [S]}{K_m + [S]}$$

In this equation V denotes the velocity of the reaction, V_{max} denotes the maximum velocity of the reaction, and K_m (Michaelis Constant) is the concentration of substrate at which the reaction proceeds at half its maximum velocity. These parameters can be seen in visual format in Figure 6 and are usually determined experimentally by exposing the enzyme to varying levels of substrate.

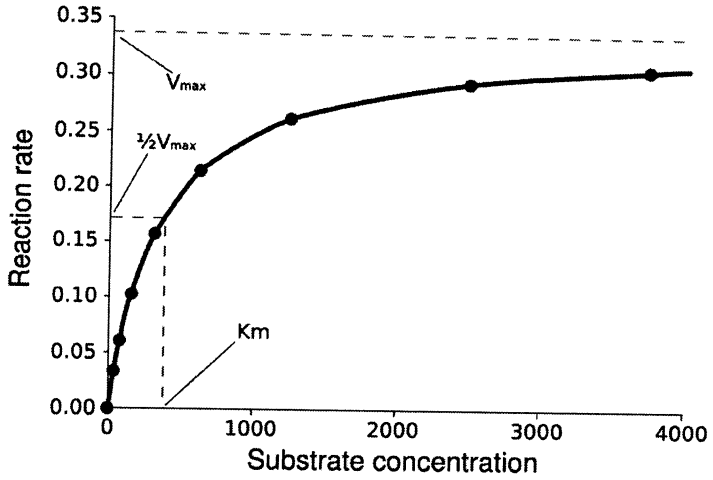

Figure 6 – Typical Graph of Cleavage Rate vs. Substrate Concentration used to calculate Michaelis-Menten Parameters

1.3. Probes for Protease Detection

1.3.1. Overview

Various approaches have been taken to the development of methodologies to assay protease activity. These various efforts can be broken down into two categories, each with distinct goals. The first is methodologies that have been developed for the purpose of research and *in vitro* applications. These have focused understanding protease function, identifying important protease markers in disease, and screening for protease substrates. The second set of methodologies is aimed at developing probes for *in vivo* detection and imaging. These approaches are based on translating protease activity into some form of optical signal and are designed to better understand protease function *in vivo* and act as prognostic and predictive markers for pathologies.

1.3.2. *In Vitro* Protease Detection

Focus in this area can be broken down into three levels: work at the transcriptional level, work at the protein level, and work at the protease activity level. Although the first two levels of detection play a role in the discovery of protease function, it is really the activity in living tissue that is important. As has been mentioned, many levels of protease control are post-translational. As such, determining the activity and not just presence of proteases in living tissues is of the greatest importance.

At the transcriptional level, much of the advances have focused on the development of DNA micro-arrays. The identification of protease coding genes[25], facilitated by the sequencing of the human genome, has led to micro-array platforms such as the Hu/Mu ProtIn Microarray[59] and the CLIP-CHIP[60]. These both rely on extracting RNA from the tissue in question, amplifying it, and hybridizing it with the microarray. Further analysis can be done with quantitative real-time polymerase chain reaction[61]. This work, however, is limited in its scope as it is only able to assay protease activity very indirectly. While allowing the detection of various mechanisms that alter transcription, such as genetic mutations in promoter sequences, this provides only a limited view of the various levels of protease control.

At the proteomic level, much of the efforts have focused on the use of mass-spectroscopy techniques[62] to achieve high throughput screening. In these systems, complex protein samples are separated by chromatography. These are then ionized using electrospray ionization or matrix-assisted laser desorption/ionization (MALDI) and analyzed by combinations of Time of Flight (TOF), ion trapping, and quadripole

analyzers. One such example is MUltiDimensional Protein Identification Technology (MUDPIT) which was proposed by Link et al[63]. While providing an improvement over methods that assay only transcription, these methodologies are also limited in their ability to assay protease activity. Many proteases that play important roles in cancer progression are naturally present and stored both in the cellular and ECM environment. It is changes that result in their activation and in the disruption of their inhibitors that allow protease activity to change.

Finally, various efforts at the cellular level have been made to survey activity. One example is the use of flow cytometry to measure cathepsin activity in cells[64]. Another technique that has been used involves the introduction of probes in plasmid vectors into cells. One group utilized such a technique to monitor MMP activity by creating a probe containing DsRed2 and cyan fluorescent protein (CFP) linked by and MMP substrate site[65] while another used a similar technique to study the role of ubiquitin[66].

1.3.3. *In Vivo* Fluorescent Probes

As demonstrated by the limitations of the methodologies surveyed in section 5.3.2, there is a great need for the development of probes that will allow *in vivo* analysis and imaging of protease activity, an indicator affected by all four levels of protease control. These techniques are essential as they allow determination of protease activity affected not only by its presence but also activation, localization, and inhibition. There are two main groups of such probes, those that detect active proteases and those that monitor protease substrate cleavage. Both approaches rely on the principle of

Förster/Fluorescence resonance energy transfer (FRET). Named after Theoder Forsrter in 1948, it describes the transfer of energy from one chromophore to another when they are in close proximity[67]. The level of energy transfer is defined by the spectral overlap of the emission of one fluorophore and absorbance of the other as well as their spatial separation. A visual representation of this effect and how it affects a sample emission spectra as well as the equation describing the level of energy transfer can be seen in Figure 7. In the equation below, *E* denotes the FRET efficiency (fraction of energy transferred), *r* is the distance between the two molecules, and *Ro* is the Forster distance (distance at which 50% of energy is transferred).

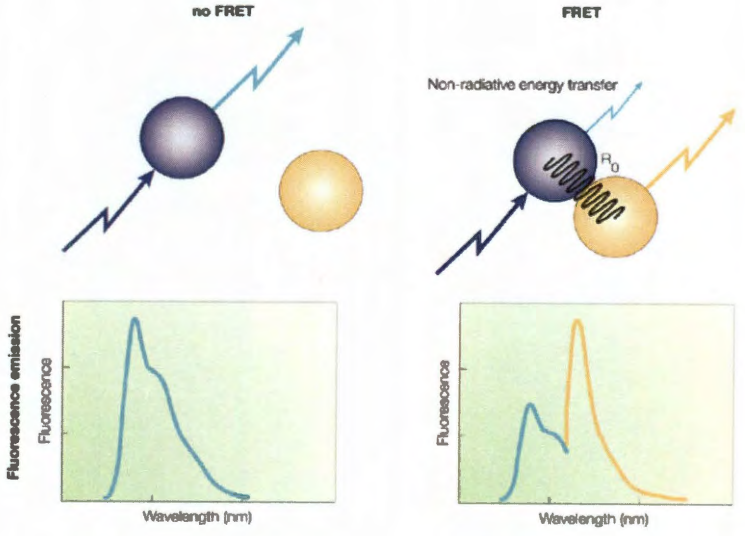

$$E = \frac{1}{1 + (r/R_0)^6}$$

Figure 7 – Forster/Fluorescence Resonance Energy Transfer

From Rudolf et al. 2003[68]

The first set of probes built on this principle is activity based probes[69]. They are generally made up of three parts. The first is a reactive 'warhead' that covalently bonds

itself to a target in question, namely an active protease in this case. This is complemented by a peptide that increases the binding specificity of the probe. The final component is a fluorophore and quencher pair. Once the probe attaches itself to the target, a reaction is catalyzed that releases the quencher. This results in an increase in fluorescence which can be measured and correlated to the level of active protease. The general design of these probes can be visualized in Figure 8. This technique has been widely applied for the detection and *in vivo* imaging of various proteases including cathepsin, MMP activity[70,71,72].

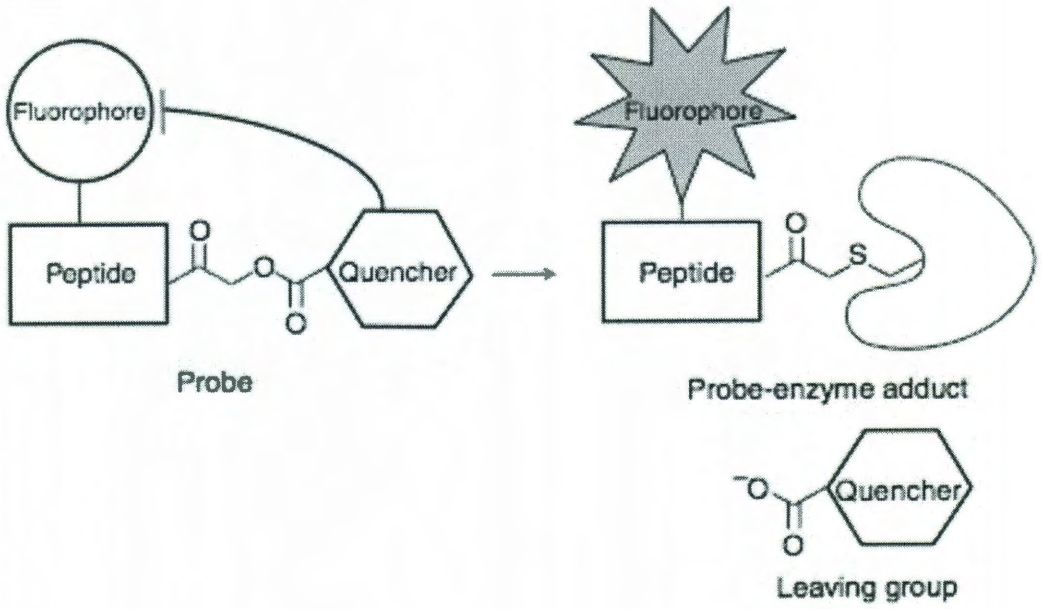

Figure 8 - Activity Based Probe Design - When the reactive 'warhead' of the probe attaches itself to the active site on the protease, it results in the release of the quencher and thus restore the fluorescence of the probe. The specifity of the probe is increased by the presence of a peptide.

From Kato et al. 2005[72]

The second group of probes is those that rely on measuring protease substrate cleavage and are the most relevant to our proposed work. This class of probes also relies

on FRET and involves the use of three main parts. They consist of a fluorophore and a quencher linked by a cleavable peptide substrate. When these probes are exposed to an active protease that recognizes and cleaves the peptide substrate, the quencher and fluorophore separate and fluorescence increases. This can be visualized in Figure 9.

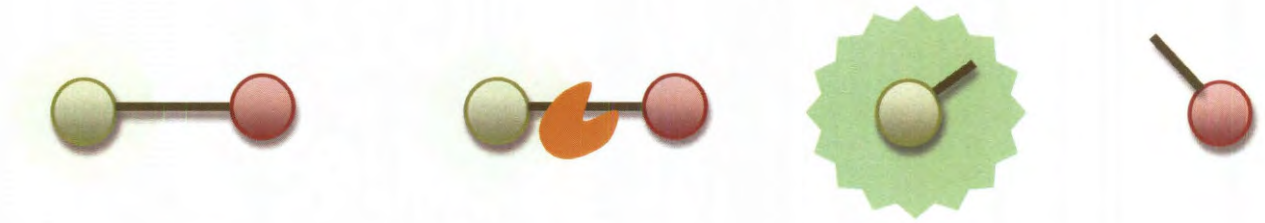

Intact Probe: Fluorescence Quenched

Protease Cleavage of Specific Peptide Substrate

Separation of 2 parts: Fluorescence Restored

Figure 9 - Principles of FRET protease probes

The choice of fluorophore and quencher varies based on the application. Several such combinations that have been used are tryptophan with dinotrophenyl[73], dinitrophenyl with methoxycoumarin[74], EDANS with DABSYL[75], and CyDye pairs such as Cy3 wih Cy5Q quencher[76]. A great deal of the functionality of the probe relies on the specific recognition and cleavage of the peptide sequence by the protease in question. As such, much attention has been given to identifying and profiling the specificity of various sequences to various proteases. An example can be seen in the development of peptide microarrays used to determine specificity[77]. These techniques have been shown to be useful not just *in vitro* but also for *in vivo* imaging of protease activity in various pathologies such as tumors[78,79] and myocardial infractions[80].

1.3.4. Limitations of Substrate Based Probes using Organic Fluorophores

Probes using organic fluorophores and quenchers suffer from a set of fundamental limitations. The first is that organic fluorophores and quenchers are sensitive to both photobleaching as well as chemical degradation[81]. As these probes are designed for monitoring and quantify protease activity *in vivo*, this can be a severe limitation. In order to try and avoid photobleaching, experiments using these probes must be done in short time frames. In addition, as the degree of photobleaching is hard to determine, quantification of protease activity is next to impossible.

In addition, the narrow absorption and wide emission spectra of organic fluorophores makes the use of multiplexed experiments difficult[81,82]. Such experiments would require multiple excitation sources and quantification of results would be made very difficult due to spectral overlap of emission spectra. It is these challenges that our proposed work is designed to address.

1.4. Quantum Dots

1.4.1. General Overview

Quantum Dots (QD) are a class of nanoparticles that have recently emerged as a very promising solution to many biological problems[83,84,85]. QD, which are semi-conductor nanocrystals, operate on the principle of quantum confinement. In bulk semi-conductor materials, electron-hole pairs are bound by the Bohr exciton radius. QD, which range from 2 to 10 nm in radius, further restrict the electron-hole pairs leading to unique optical and electrical properties. QD absorb photons of light anywhere at or

below their first absorption peak and release the energy in excitonic fluorescence. The position of this sharp emission peak on the spectrum is tunable and dependent on the size of the QD. Figure 10 demonstrates the various the absorption and emission spectra for particles of various sizes. It is these unique optical properties which give QD many advantages in biological applications and make them ideal for the proposed work.

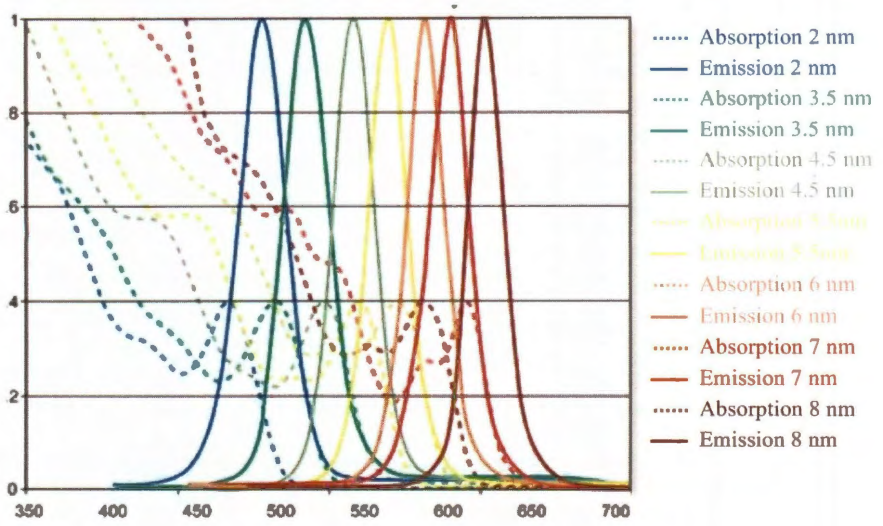

Figure 10 - Absorbance and Fluorescence of QD of various sizes

Modified from Portney 2006[86]

QD are generally composed of elements from the periodic groups II–VI (such as CdSe, CdTE) or III–V (such as InP).[87] While this semiconductor crystals provide the effects described above, two modifications are required for use in biological systems. The first of these is the capping of the QD with a high band-gap material[88,89]. This cap allows the quantum yield of the QD to be increased while simultaneously providing a layer of protection to the biological system from the toxic elements that make up the core crystal. In addition to a cap, QD require a water solubilization coating which both further protects the QD and allows the use of QD in aqueous environments[90].

1.4.2. Advantages of Quantum Dot

The unique properties of QD present many advantages over organic fluorophores in designing a system to monitor protease activity. The first of these is the ease of creating a system of probes with orthogonal emission peaks that can easily be differentiated. QD have sharp emission peaks whose positions are easily tunable. In addition, the existence of multiple energy states in QD allows them to be excited at any wavelength below the absorbance peak[87]. In comparison, organic fluorophores generally possess broader emission spectrums with a long tail at red wavelengths. In addition, the excitation spectrum for organic flurophores is generally very narrow. Thus, a system utilizing QD would need only one excitation source, allow numerous proteases to be studied, and would produce readings that could easily be quantitatively analyzed. The use of organic fluorophores would however necessitate multiple excitation sources and possess limited multiplexing ability.

The second major advantage QD present is their greatly decreased sensitivity to both photobleaching and chemical degradation[91,92]. Conventional organic fluorophores are very sensitive to photobleaching and as such are not suitable for long-term imaging. This can be seen in Figure 11. In addition, properly coated QD are protected from chemical degradation in harsh salt conditions (0.01 to 1 M), a wide range of pH (1 to 14), and even after harsh treatment with 1.0 M hydrochloric acid[93].

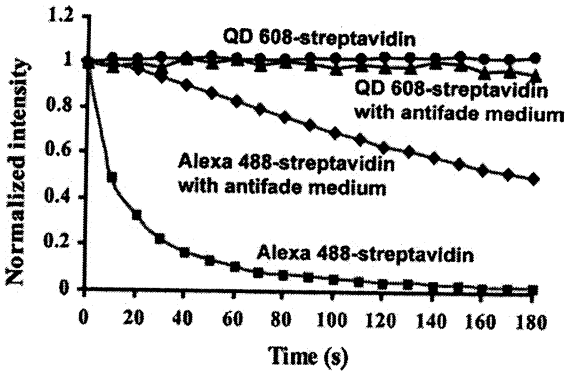

Figure 11 - Photobleaching Resistance of Quantum Dots

From Alivisatos et al. 2005[87]

The third major advantage of QD for our application is that of their size. The range they are in allows for multiple fluorescence quenchers to be attached to each particle. In addition, their bigger size with respect to organic fluorophores allows for better control over their cellular distribution. QD have been shown to behave much like fluorescent proteins and do not suffer from any limitations in terms of steric hindrance or binding kinetics[94]. In addition, due to their intermediate size range, QD are small enough to reduce reticuloendothelial uptake and phagocytic opsonization while being large enough to avoid renal filtration[95]. Finally, due to their size, QD can accumulate in tumor tissues with passive targeting through the enhanced permeability and retention effect[96].

1.4.3. Various Types of Quantum Dots and choice of CdSe

As discussed earlier, QD can be made with pairs of various elements in the periodic groups II–VI or III–V. Examples of these include but are not limited to CdS, CdSe, CdTe, PbSe, InP, and CdHgTe. While these QD possess similar properties they vary mainly in the size-dependence of their emission peaks. This size dependence can be seen for various types in Figure 12.

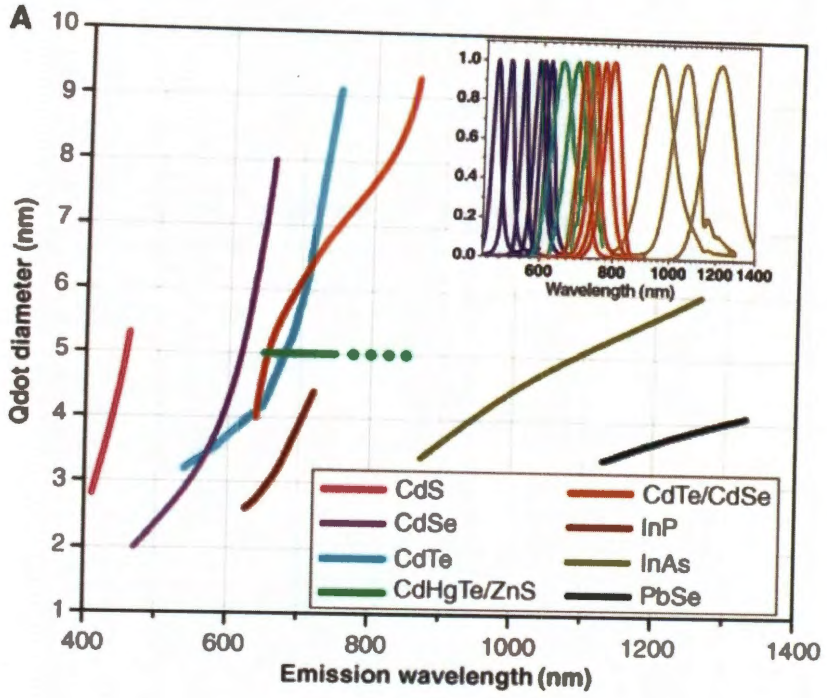

Figure 12 - Various Types of Quantum Dots and their Size Dependant Emission
From Michalet et al. 2005[89]

The choice of which of these particles to use is based on the application that is needed. Figure 13 overlays the spectra of various forms of QD with various biological applications. Monitoring protease activity *in vivo* at depths great than 500 μm requires the use of NIR light in the 650-950 nm range[97]. This constrains the choice of QD for our application to CdSe and CdTe QD. Of the two, CdSe have the advantage of being also found in the visible range. This allows initial characterization and *in vitro* studies to be undertaken with greater ease.

In addition to spectral considerations, the level of research in terms of synthesis strategies and cytotoxicity must also be considered. The various synthesis strategies that have been developed for water-solubilization and that have shown promise in various *in vivo* applications have mainly involved the use of CdSe QD. Likewise, evaluation of QD

cytotoxicity has focused on CdSe QD. As such, all efforts will involve the use of CdSe QD. The development of probes further into the NIR range could eventually be done by using the CdTe QD.

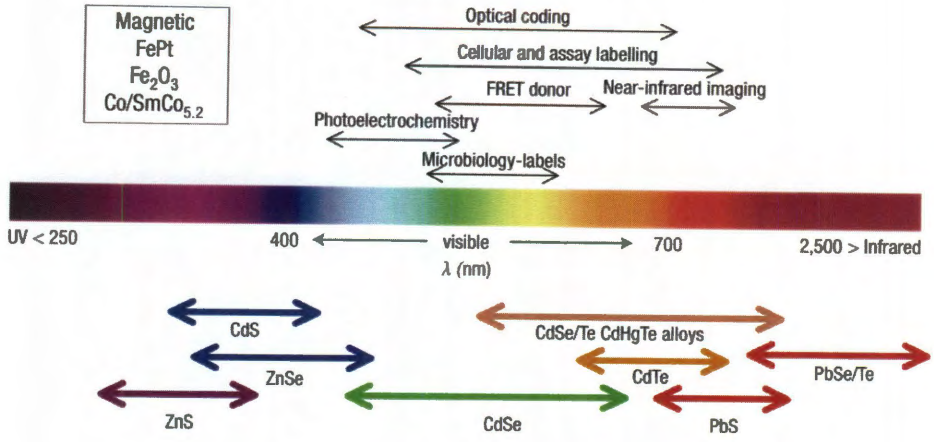

Figure 13 - Location on Spectrum and General Usage in Biological Systems

From Igor et al. 2005[90]

1.4.4. Water Solubilization of Quantum Dots

The use of QD in biological applications necessitates the use of some form of water solubilization. This coating has three main tasks. First it allows the QD to be soluble in biological aqueous environments. Second it provides further protection to the QD against degradation improving cytotoxicity. Finally, it provides a scaffold that can be used to further functionalize the particle. In addition to these basic properties our proposed work requires that the coating be thin enough to allow quenching of particle fluorescence and at the same time maintain the full fluorescence of the particle.

Many techniques have been employed to achieve this purpose. These fall into three main categories. The first of these is surface-ligand exchange. In this group of

methodologies, the TOPO coating of QD is replaced by bio-compatible ligands. Examples of these include the use of mercaptocarbonic acid[98], mercaptoacetic acid[99], bidentate ligands[100], and dihydrolipoic acid derivatives.[101] The drawback to most of these methodologies is that the surface exchange usually results in a decrease in the quantum yield of the particles and thus counteracts one of the benefits of using QD.

The second general strategy for solubilizing QD is to create silica shells that act as an insulation. Various groups have demonstrated these techniques with the use of mercaptopropyl silanols[92,102] and tetraethyl orthosilicates[103]. While these show great stability and even enhance fluorescence, they have one main drawback for our applications. The size of the shells being produced has a thickness of 5-30 nm. This size of the resulting QD greatly limits their application as quenchable particles since quenching of fluorescence varies with separation of the quencher and fluorophore.

The third main group of strategies is the use of amphiphillic polymers which coat the surface of the QD. These strategies rely on a tight encapsulation of the QD by the polymers due to hydrophobic interactions. The resulting QD are composed such that the hydrophobic portion of the coating tightly interleaves with the TOPO coating and leaves the hydrophilic outer groups on the outside to allow solubility in water and further functionalization. Various strategies have been employed including amphiphillic triblock copolymers[104], poly(maleic anhydride-alt-1-tetradecene) (PMAO)[105], amphiphillic sacharides[106], and a modified acrylic acid polymer[107]. These strategies have the advantages that they produce a rather thin coating, do not affect QD fluorescence, and can easily be functionalized. For these reasons, this class of water solubilization will be

chosen for the proposed work. Work will mainly focus on the use of the amphiphilic triblock copolymers as well as PMAO.

1.5. Imaging of Quantum Dots

1.5.1. Overview

Due to their many benefits, a great deal of attention has been focused on the utilization of QD for *in vivo* and *in vitro* optical imaging. This work has helped to identify some of the characteristics that define the behavior of QD in biological environments. These will be important to understand and build upon in the proposed work.

1.5.2. *In Vitro* Imaging

In vitro imaging of cells has focused on two main areas. The first is the development of QD for the labeling of cell-surface receptors. This has allowed study of the function, internalization, and distribution of various membrane receptors including the ErbB/HER receptor protein-tyrosine kinase[108], glycine receptors[109], and integrins[110]. An overview of the methodologies used for this type of targeting can be found in Jaiswal et al.[111] and imaging in these works was conducted with both confocal and epifluorescence microscopy.

The second area of focus of *in vitro* imaging of QD has been developing methodologies for their intracellular delivery. Initial attempts hoped to take advantage of passive endocytosis[112]. Although somewhat successful, the resulting QD remained localized in vesicles. Other attempts were made at using membrane-receptor signals to

induce uptake[113]. This was shown to occur by activation of signaling pathways and also indirectly by increasing the QD concentration near the surface of cells. Two alternative techniques, micro-injection[114] and electroporation[115], have also been studied. While micro-injection has been shown to be quite successful, having been able to encapsulate over $4x10^9$ QD per cell, this technique is limited as it requires cell by cell processing.

To achieve more direct uptake, another set of efforts has focused on using peptides directed at the twin-arginine translocation (Tat) pathway. This methodology, which results in macropinocytosis[116], has been studied using spinning dark confocal microscopy to follow the QD post uptake[117]. A lot of the above mentioned methods result in the accumulation of QD in cellular vesicles. As such, a final set of attempts has used polyethylenimine-PEG as an endosome-disrupting agent to allow cytoplasmic distribution of QD[118].

1.5.3. *In Vivo* Imaging

More relevant to our work is the use of QD for *in vivo* imaging. This work demonstrates some of the challenges and components that must be considered when utilizing QD for *in vivo* imaging. One of the initial *in vivo* applications of QD was in a frog embryo model by Dubertret et al.[119]. It was shown that with the use of proper water solubilization protective coatings, QD could be used to image embryo development for up to four days with no cytotoxicity. Following this success, several groups have reported successful use of QD in mouse models. The work of Ballou et al. demonstrated general behavior of injected QD in live mice including circulation times and tissue

distributions using both whole-body imaging and microscopy of tissue samples[120]. Subsequently, Voura et al. utilized QD in order to track metastatic tumor extravasation *in vivo*[121]. Though this demonstrated the utility of QD in understanding *in vivo* behavior, imaging of these specimens was performed after the sacrifice of the animals.

One of the first successful demonstrations of QD for *in vivo* imaging and detection of tumors was performed by Gao et al.[96] In this paper, they demonstrated the utility of QD to successfully image tumors *in vivo*. Two forms of tumor targeting were investigated as seen in Figure 14. The first was passive tumor targeting in which QD accumulate in the tumor solely by the EPR effect. The second, active targeting, involved the conjugation of the QD to cancer specific antibodies (Prostate-specific membrane antigen PSMA). These antibodies, which are conjugated onto free COOH groups of the amphiphilic polymer coating, help to increase tumor QD accumulation by allowing the QD to rapidly binding to tumor-specific antigens.

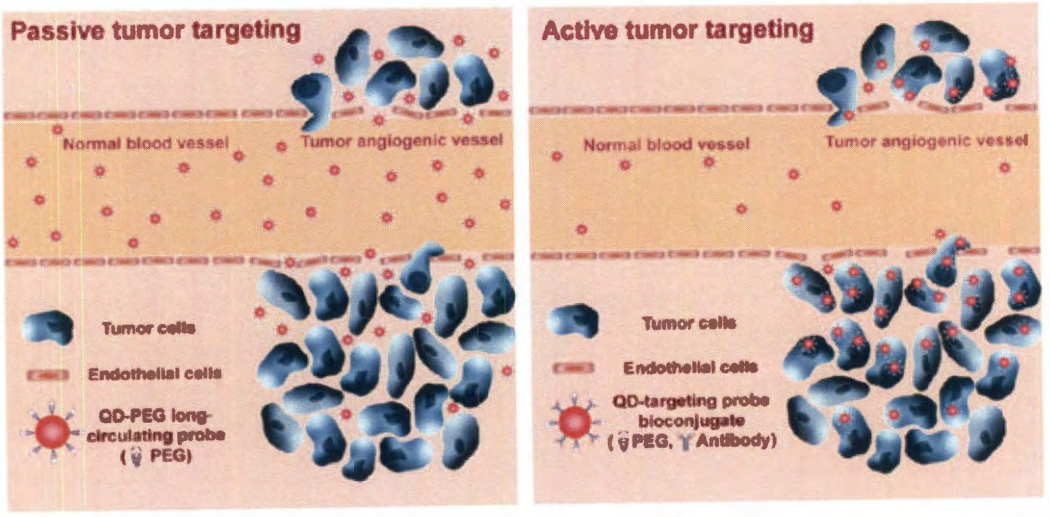

Figure 14 - Active and Passive Targeting of QD

Modified from Gao et al. 2004[96]

The results of tail veil injections on the biodistribution of the QD were examined as seen in Figure 15. In section a, QD-COOH and QD-PEG were injected at 6 nmol via tail vein and images are after 24hrs, while QD-PSMA were only injected at 0.4 nmol and imaged after 2 hr. Section b shows results when all three groups were injected at 0.4 nmol and imaged after 2 hr. As can be seen by the tumor images in section a, tumor accumulation was heightened by active targeting. This is shown by the fact that an injection of 1/15 as many targeted QD produced a better image after 2 hr than did only PEG-coated QD after 24hr. Of interest, however, is the fact that even at 2 hr, passive targeting of QD did produce some signal in the tumor as seen in section b.

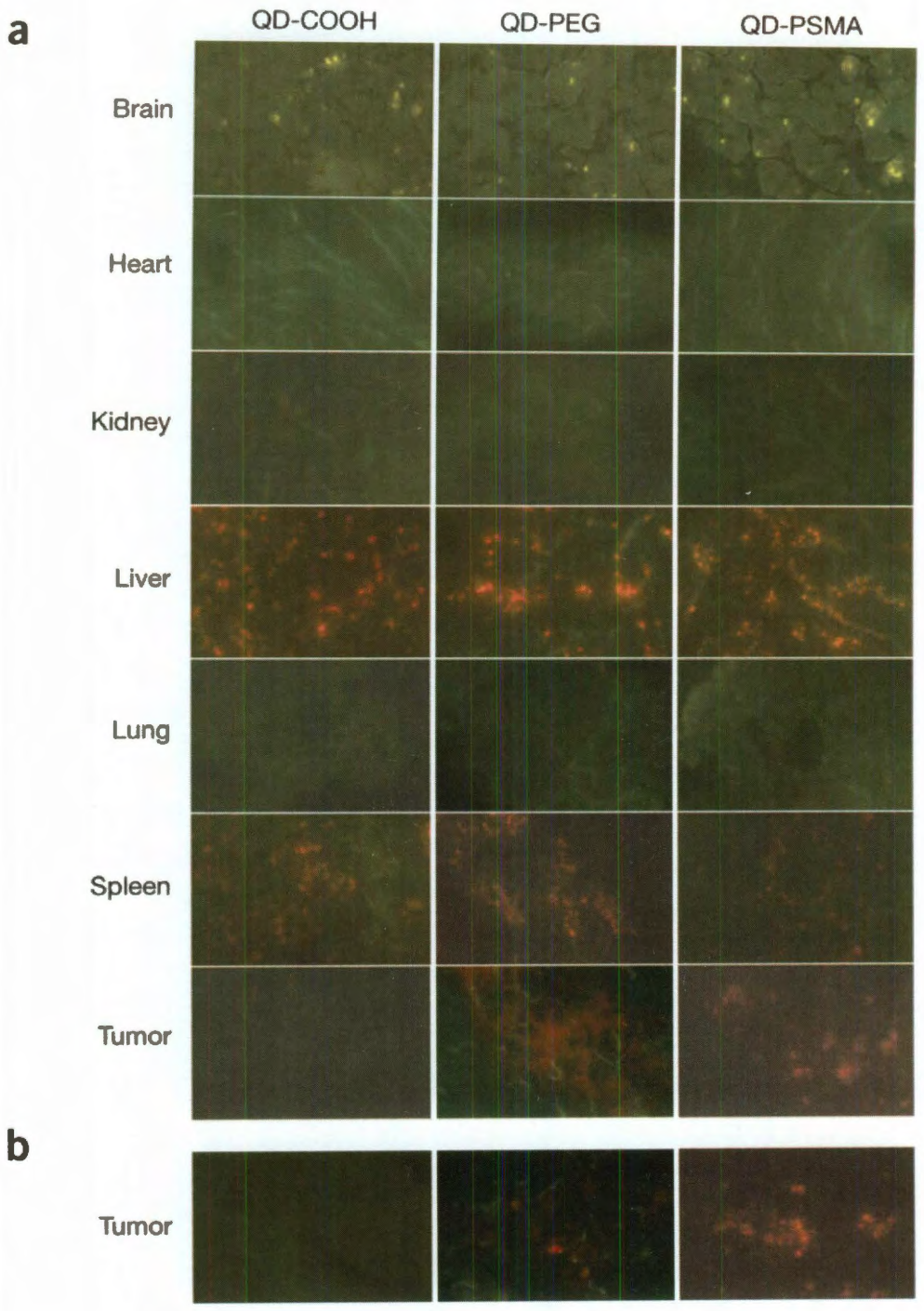

Figure 15 - Biodistribution of QD in various tissues - Green represents tissue autofluorescence while red represents signal from QD. Images are of 5-10 μm sections taken with epifluorescence microscopy.
From Gao et al. 2004[96]

In addition to the ability to determine biodistribution in the mice, whole-body imaging was performed and demonstrated the ability to detect tumor location as seen in Figure 16.

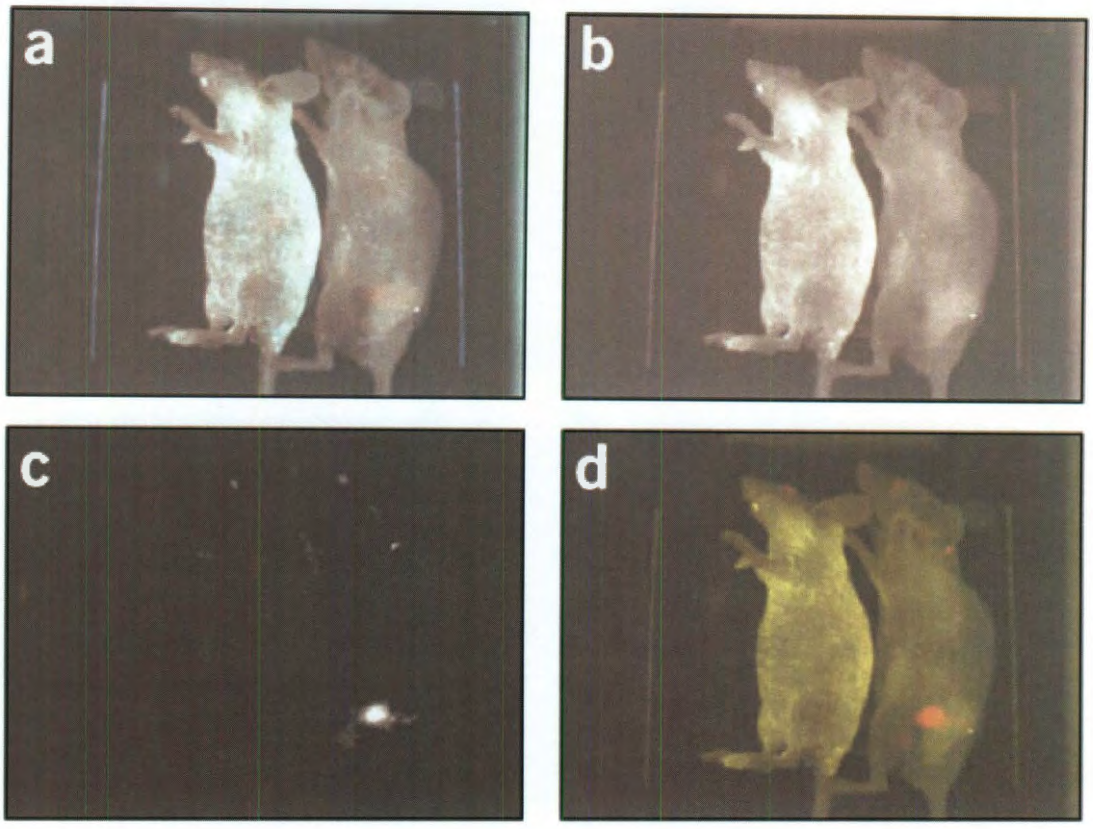

Figure 16 - Whole-Body Imaging to Detect Tumor Location - Panel a represents the original picture taken. Using spectral unmixing algorithms, mouse autofluorescence, panel b, and QD signal, panel c, were separated. Panel d represents the overlap of mouse autofluorescence (yellow) and the tumor (orange).

From Gao et al. 2004[96]

This work demonstrated the ability to get QD accumulation in the tumor, whether through passive or active targeting, and visualize them using whole-body imaging, laying the foundation for the *in vivo* studies in the proposed work.

1.6. Protease Probes using Quantum Dots

1.6.1. Overview of Quantum Dot attempts

QD are currently being investigated in a variety of biological applications including small molecule biosensors, measuring peptide-RNA interactions, and targeting cell surface receptors[122]. Directly relevant to the proposed work, initial attempts have been made to utilize QD for the monitoring of protease activity[123,124,125,126]. The general design for the various probes has been similar in nature. A Cd/Se QD is used as a fluorescence source and is rendered water soluble. A degradable peptide linker is then used to attach some form of quenching molecule.

The various approaches described above vary mainly in three aspects. The form of water solubilization used, the choice of quencher molecule, and the linker used. The various water solubilization methods that have been used are DHLA[126,124] and streptavidin[125]. The quenchers they chose to use were rhodamine[124], Cy3, and dark quencher QXL-520. These attempts have been successful at demonstrating the utility of this form of probe.

1.6.2. Quantum Dot Quenching with Gold Nanoparticles

As an alternative to the use of organic quenchers, the proposed work chooses to use AuNPs to obtain quenching. Many groups have shown the ability of AuNPs as quenchers for organic dyes[127]. In addition, recent work has shown that AuNPs can serve as optical quenchers for QD[128]. Figure 17 demonstrates the quenching ability of just one AuNP linked to a QD.

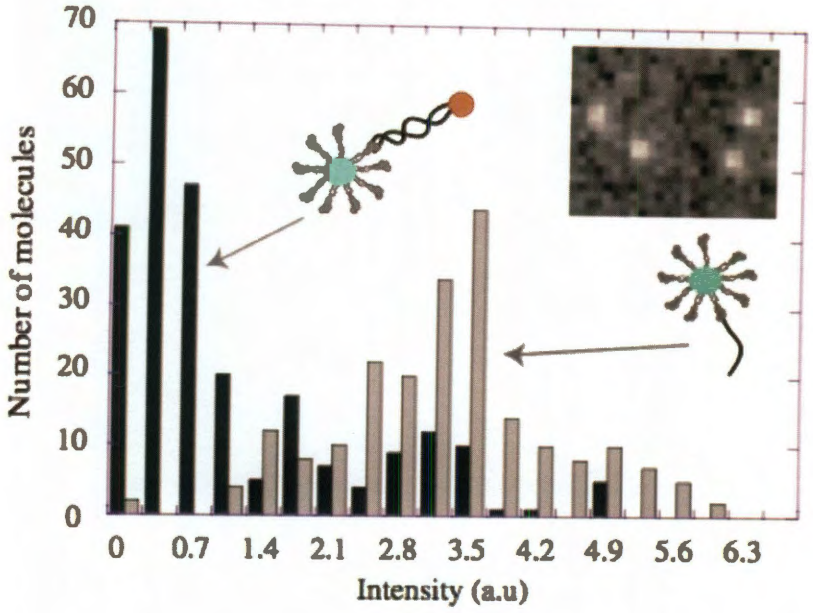

Figure 17 - Optical Quenching of QD by a gold nanoparticle - Histograms of the intensity within the QD for both gold-quenched (seen in black) and unquenched (seen in gray). Pictures were taken using epifluorescence microscopy of QD adsorbed onto a glass surface.

From Gueroui et al. 2004[128]

1.6.3. Initial Work

Two groups have successfully demonstrated at a proof of principle level the quenching of QD with AuNPs[129,130]. In 2005, Chang et al. assembled a QD protease-activated probe[129]. The general functionality of the probe can be seen in Figure 18.

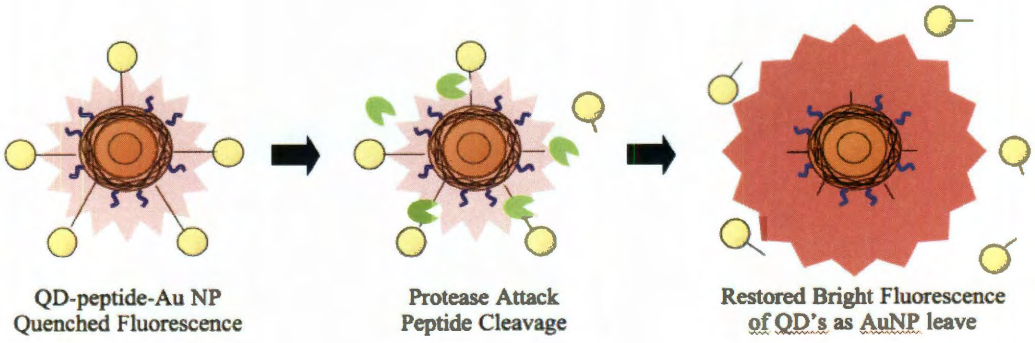

Figure 18 - Protease-activated Quantum Dot Probe

This work utilized Cd/Se Cd/S QD coated with a PMAO water solubilization coating. This PMAO coating was further functionalized by the addition of poly(ethylene glycol) to increase water solubility and stability. The resulting QD were then conjugated to a degradable peptide sequence GGLGPAGC. Mono-maleimide functionalized AuNPs were then attached to the QD via the cysteine residue on the conjugated peptide. A control group was also created in which all steps were carried out except for AuNP attachment. An initial study demonstrated that the protease-activated probes had been quenched by 71% as can be seen in Figure 19.

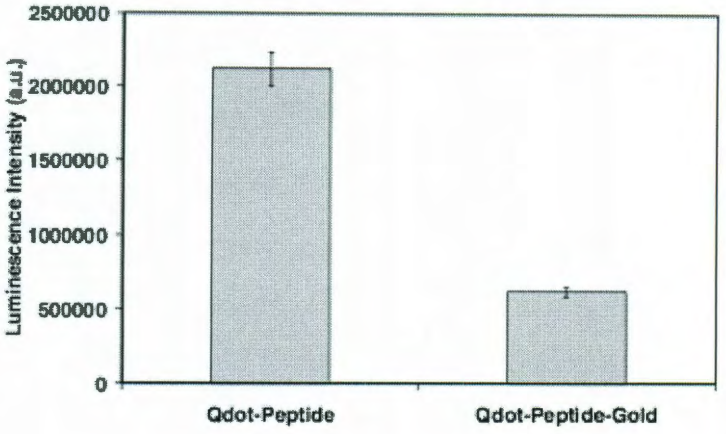

Figure 19 - Quenching of QD by AuNP

From Chang E. et al. 2005.[129]

This demonstration was followed by a study to determine the ability of the probes to regain their fluorescence upon exposure to collagenase. The results of this study can be seen in Figure 20. The probe was incubated with 0.2 mg/ml of collagenase and with water as a control. In addition, auto-fluorescence measurements were taken for collagenase to use as a baseline for fluorescence. The study showed a 52% recover of fluorescence at the 47 hr time point.

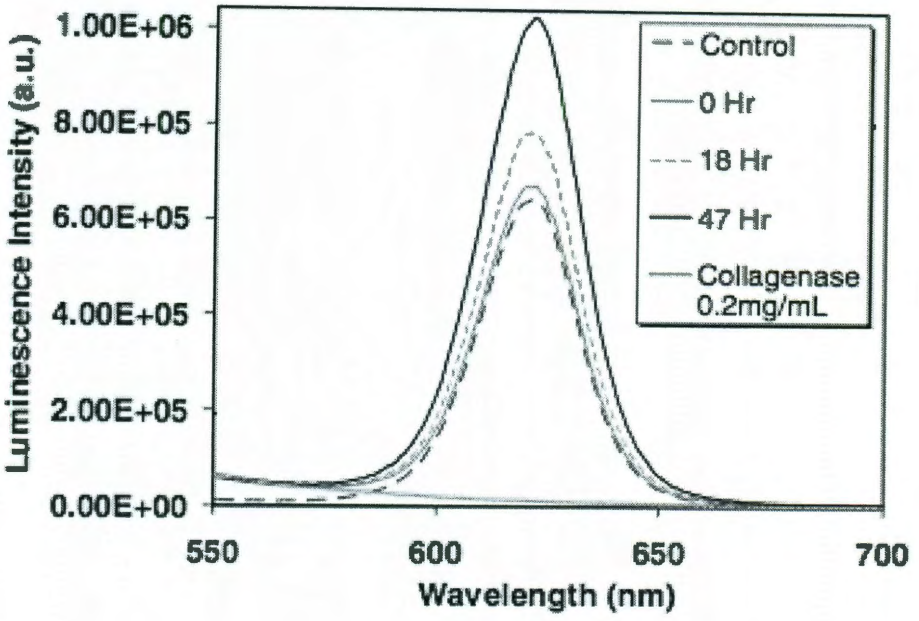

Figure 20 - Qd Probe Fluorescence recovery - Fluorescence recovery due to peptide linker cleavage was measured in the presence of 0.2 mg/L collagenase in HBS and HBS control. Collagenase autofluorescence was also measured to calibrate against.

From Chang E. et al. 2005.[129]

In addition to this effort, Kim et al. also demonstrated the functionality of such QD – AuNP conjugates[130]. They utilized a similar approach and demonstrated its application as a multiplexed assay by conjugating the probes onto a surface.

1.7. Project Summary

The development of a tool that would allow one to assay the activity of multiple proteases in real time, with ease of quantification, and in live tissue is a goal that holds great potential. QD, who possess both the stability and narrow emission peaks required, were used to create probes that held such promise. By linking the fluorescent QD to shield-like AuNP via protease degradable linkers, protease-activated quantum dot probes were fabricated. These probes, whose emission properties can easily be tuned via the size of QD used, are both stable and easily quantifiable. In the presence of active proteases, the linkers are cleaved, AuNP are released, and the QD fluorescence is restored.

To construct an optimized probe, both linker length and AuNP:QD ratio were investigated to determine their effect on fluorescence recovery. Since both an increase in AuNP:QD ratio and decrease in linker length cause greater quenching (potential for recovery) while simultaneously decreasing protease access, an optimum balance needed to be found.

Finally, with optimization complete, two probes with orthogonal emission spectra (sensitive to either cathepsin K or collagenase) were fabricated. It was demonstrated that one could use these two probes simultaneously to monitor proteolytic activity.

Chapter 2: Materials and Methods

2.1. Synthesis of Poly(acrylic acid)-Oleylamine Water Solubilized QD

Water solubilized QD required for production of the probes were synthesized by forming Cd/Se cores, adding Zn/S shells, and solubilizing these with a poly(acrylic acid)-oleyl amine (PAA-OA) coating. These processes are outlined below.

2.1.1. Cd/Se Core Synthesis

Cd/Se Core synthesis was undertaken using a methodology previously reported by Li et al.[131] Before beginning the reaction a stock solution of 1:1.2:2.7 molar ratio Se(99.5%):tributylphosphine(97%):1-octadecene was prepared. The initial stage of the reaction involved 0.4 mmol of CdO (99.99%), 1.6 mmol of stearic acid (99%), and 4g of ODE in a 50ml 3-neck flask. This mixture was heated to about 180 °C or until the solution became clear. The solution was then cooled to room temperature.

Then 1.5g of ODA (97%) and 0.5 g of TOPO (90%) were added. The 3-neck flask was filled with argon and heated to 280 °C. As soon as this temperature was reached, a volume containing 2 mmol of Se of the Se-TBP solution is injected. The reaction was terminated, resulting in a stop of growth in size of the QD, by pouring the resulting liquid into a solution of hexane or chloroform. Resulting particle size was controlled by varying the time in between Se injection and quenching of the solution, with 15s producing green QD to 3-4 min producing red QD. Initially, small reactions were undertaken with small withdrawals of the solution at various time intervals to determine the time-dependency of the size of the QD. With this determined, the entire

batch was quenched at once at a given time point to produce large numbers of QD. These cores were then cleaned as outlined in section 2.1.3.

2.1.2. Zn/S Shelling

In order to shell Cd/Se particles with Zn/S, QD concentration and size were determined. Particle size was obtained by measuring peak absorbance on a UV-Vis spectrophotometer between 400-800 nm. This absorbance spectrum was used to calculate size using standard curves published by Yu et al.[132] as seen in Figure 21 where the X-axis denotes the peak absorbance.

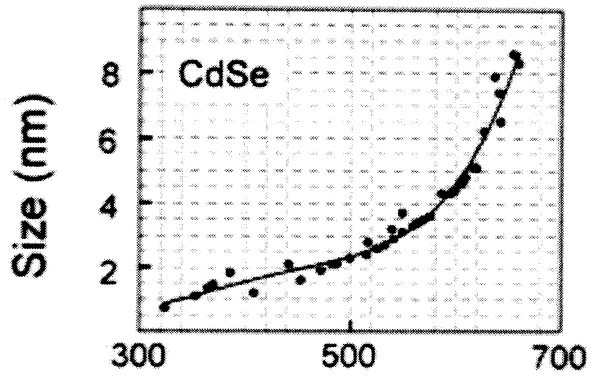

Figure 21 - CdSe standard Curve for Size vs. Peak Absorption From Yu et al. 2003[132]

QD particle concentration was determined in two ways. The first method was to use the empirical fitting of concentration to absorbance as described by Yu et al.[132]. In their model, $A=\varepsilon CL$ and $\varepsilon=5857(D)^{2.65}$ which leads to $C=A/(L*5857(D)^{2.65})$. In this model A represents absorbance at peak, C represents concentration, L is the path length of the beam measuring absorbance, and D is the diameter of the QD. While this method yielded good estimations of concentration, more precise concentrations were obtained by

performing Inductively Coupled Plasma with Optical Emission Spectroscopy (ICP/OES) as described in section 2.2.3.

Having determined size and concentration of QD, calculations were undertaken to determine the amount of reagents needed for each shelling layer. This calculation was made using the knowledge that each ZnS layer was approximately 0.35 nm. Based on the change in volume produced by each layer and the density of both Zn and S, amounts for each shell were calculated. Shelling of the particles was undertaken using the method described by Li et al.[133]. 0.04 M solutions of both ZnO and S were prepared. ODA and ODE were added to the QD to be shelled, currently in hexane in a 3-neck flask. The solution was placed under vacuum and heated to 100 °C to remove the hexane. Once complete, the flask was placed under argon flow and heated to 200 °C. Once this temperature was reached, an injection of the volume required for the first Zn shell was added. To determine when to add the next layer, UV-Vis readings were taken until there was no longer a shift in the peak absorption. This was repeated until the QD were shelled with three layers.

2.1.3. Cleaning of Cd/Se cores and shelled QD

In order to accomplish the cleaning of the particles after both core synthesis and Zn/S shelling several methodologies were combined and modified. The final cleaning protocol involved two cleaning procedures performed one after the other. In the first stage, an equal volume of methanol was added to the hexane containing the QD. In the first few washes, the presence of various side products required centrifugation at 3000 r.p.m. for 5 min. to achieve separation. The top hexane layer was collected and the

process was repeated several times until the precipitate decreased in quantity and had little fluorescence left. In addition, for maximum yield, the precipitates were themselves re-dissolved in hexane and undergo the same cleaning procedure to extract the majority of QD.

Once the hexane/methanol cleaning was completed, a further washing step was required. In the initial step an equal volume of ether was added to the QD currently in hexane. Ethanol was then added until flocculation was observed. The resulting mixture was then centrifuged at 3000 r.p.m. for 5 min yielding QD in precipitated form. The supernatant was taken off and discarded and the QD were re-suspended in chloroform. Again a 1:1:2 mixture of chloroform:ether:ethanol was made, and centrifuged. This was repeated until the precipitate three times. After the final centrifugation, the QD were stored in the chloroform for storage.

2.1.3. PAA-OA Water Solubilization

PAA-OA solubilization was performed using 5k PAA as described. PAA was reacted with oleylamine in chloroform overnight using EDC as an activator for the carboxyl group. The molar ratio of PAA:OA used was 1:10. Upon completion, a solution of QD was prepared in chloroform. The PAA-OA polymer was added at a an excess (over 100:1 PAA-OA:QD molar ratio) and was allowed to stir overnight. An equal volume of water was then added and the solution was vacuum dried using Rotary Evaporation (Rotovap) to remove the chloroform. The final product was centrifuged using an ultra-centrifuge at 200,000 g for 3 hr to remove excess polymer.

2.2. Characterization of Quantum Dots

The trend in recent literature involving QD is to ensure adequate characterization of all stages of QD synthesis. This requires the determination of several key characteristics of the QD at each stage of the synthesis. Once cores are produced, their size, their concentration, as well as their absorbance and emission spectra must be obtained. Similarly, this must be repeated following QD shelling. The sections to follow describe the methods involved in determining each of these characteristics.

2.2.1. Absorbance/Emission Spectra

Absorbance spectra were captured on a Varian Cry300 Bio UV-Vis Spectrophotometer. The UV-Vis was first calibrated to the solvent in which the QD were suspended. Then absorption scans were taken from 400-800 nm. Emission spectra were collected for the particles using a SPEX FL3-22 Fluorimeter. QD were excited at 360 nm and emission scans were collected between 400 to 700 nm. Bandpass slits and integration time were set to 3 nm/3 nm and 100 ms.

2.2.2. TEM Imaging: Determining Size

Size of the QD particles was determined by TEM imaging of the cores, the shelled QD, and following water-solubilization. TEM images were taken with a JEOL 2010 Transmission Electron Microscope.

2.2.3. ICP/OES: Determining Concentration

In order to determine QD concentration at the various stages of synthesis ICP/OES was used. 100 μL of QD were added to 400 μL of trace grade nitric acid. The

solution was stirred at medium speed and at 60 °C for five minutes until the solution goes colorless. The solution was then transferred to a volumetric flask and diluted with 10 mL of MilliQ water. Standard solutions of 0, 1, 5, 10, 15, and 20 ppm of Cd were prepared. A Perkins Elmer Optima 4300 DV ICP-OES was then used to determine the concentration of the prepared digest. Initial concentration of the particles was then calculated using dilution factor and particle size.

2.3. Gold Nanoparticle Formation

AuNP of approximately 4 nm were synthesized as described by Duff and Baiker[134]. Initially, 33ml of deionized MilliQ water were combined with 400 µl of THPC. In preparation for the next step, 180 ml of MilliQ water are cooled to 7-8°C. This chilled water was vigorously stirred and 4 ml of the prepared THPC solution was added. Having let the solution stir for 5 min. 6.75ml of 1% chloroauric acid (99.999%) was added. The solution was then cooled and stored at 4°C. Size of the gold colloid was monitored via UV-Vis absorbance as seen by a shift in peak absorbance as nanoparticle size increases.

2.4. Peptide Synthesis

Fmoc solid phase peptide synthesis involves the one by one addition of amino acids to a polystyrene bead resin. At each stage, an Fmoc protected amino acid is added to the growing peptide chain. The protecting group ensures that only one amino acid is added at a time. Excess amino acids are then washed away and de-protection of the Fmoc group takes place. This general schematic is seen in Figure 22.

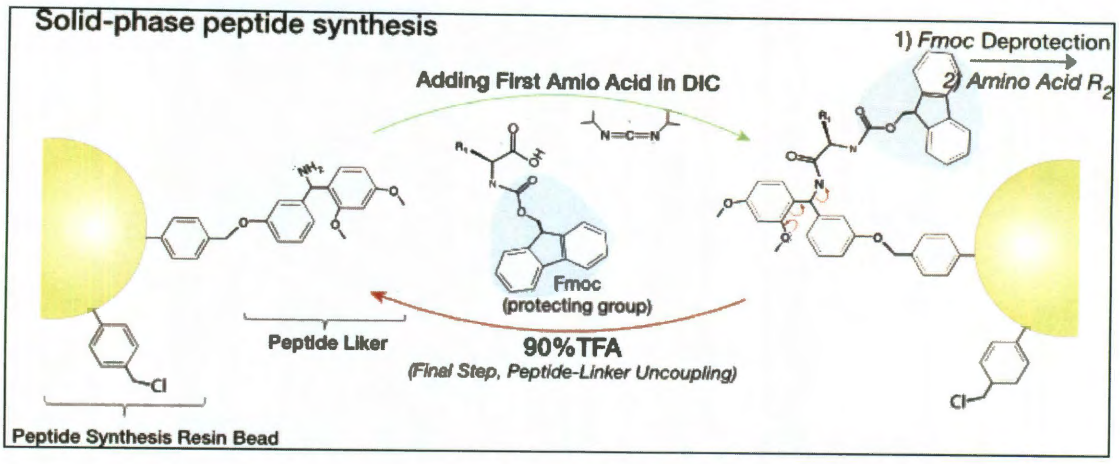

Figure 22 – Fmoc Solid Phase Peptide Synthesis
Modified from Cojocari 2009[132]

The collagenase degradable sequence XLGPAXC (X representing varying number of glycine spacers) and cathepsin K degradable sequence GGGMGPSGPWGGC were synthesized using Fmoc solid phase peptide synthesis. The collagenase sequence was chosen as it has been demonstrated to undergo cleavage by collagenase as it mimics the collagen repeat sequence -Pro-X-Gly-Pro- (where X can be almost any Amino Acid)[135]. The cathepsin K sequence chosen was used as it has been demonstrated to be an effective sequence for cathepsin K as validated by members of the lab and the MALDI-TOF results.

The collagenase and cathepsin K degradable peptides were synthesized on an automated peptide synthesizer (AAPTEC). Upon completion of the synthesis, cleavage from the polystyrene resin was done using 95% TFA (tri-fluoracetic acid), 2.5% water, and 2.5% TIPS (triisoproplysilane). The scavenger EDT (ethanedithiol) was then added to a final concentration of 2.5% to ensure deprotection of the cysteine protecting group.

Following cleavage, the water and acid were removed via rotary evaporation (Buchi Rotavapor R-200). The remaining solution was then precipitated in chilled anhydrous ethyl ether (Fisher Scientific) and transformed into a pellet via centrifugation (5 min @ 2000 r.p.m). The pellet was dissolved in chloroform and the process was repeated four times to ensure removal of residual cleavage cocktail. The final pellet was left to dry overnight, dissolved in water and dialyzed against MilliQ water using a membrane with mesh size of 500 Da (8 hr, water changed every 2 hr). The final step was to freeze the peptide at -80°C, lyophilize it, and store under argon.

2.5. MALDI-TOF Analysis of Peptides

Peptides were analyzed using MALDI-TOF to ensure proper peptide synthesis. Solutions of peptides were created at a concentration of 10 μM. Solutions were spotted onto a Prespotted AnchorChip 96 Set For Proteomics at a volume of 0.5 μL. Measurements were taken on an Autoflex II TOF/TOF. Results were calibrated using the peptide standards found on the plate. Approximately 500 shots were taken at a laser power of 22% in the range of 500-2000 Da.

2.6. Probe Asssembly

The protease-activated QD probes designed have three functional elements: QD, a peptide linker, and AuNPs. In addition, both the QD and AuNP surface must be further protected by the addition of PEG. The process of assembling the probe is outlined below.

2.1.1. Peptide Linker Addition

The first stage in probe assembly is the addition of peptide linkers the QD surface. In the case of the optimization studies the collagenase degradable peptide linkers[136,137] XLGPAXC (X representing varying number of glycine spacers) were used. Later work involving multiplexed probe also used the cathepsin K sensitive GGGMGPSGPWGGC sequence. Free carboxylic acids on the PAA polymer coating were activated to produce ester leaving groups with the use of 1-ethyl-3-(3-dimethylaminopropyl) carbodiimide (EDC) and sulfo-N-hydroxysuccinimide (sulfo-NHS) via the reaction scheme seen in Figure 23. Before addition of the peptide linker, 2-mercaptoethanol was used to deactivate excess EDC and prevent peptide linker polymerization. Peptide linkers were then added at the desired molar ratios and the conjugation was allowed to proceed overnight at room temperature. The resulting reaction mixture was dialyzed against a 10000 molecular weight cut off cellulose ester membrane to remove excess reagents and unreacted peptide. The particles were further purified and concentrated using a 50 kDa cutoff centrifugal filter (Amicon).

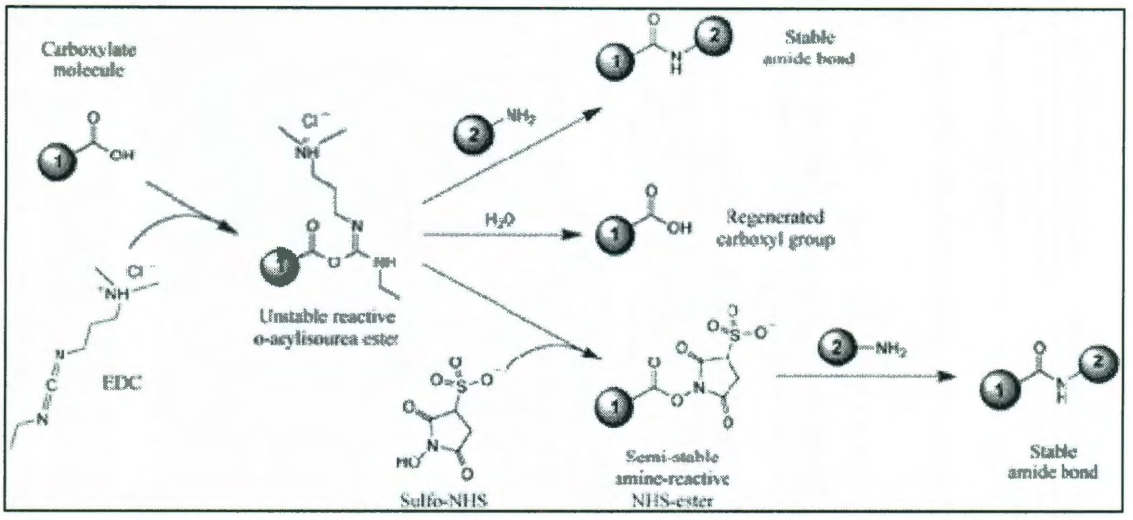

Figure 23 - General Reaction Mechanism for EDC/ Sulfo-NHS mediated Amide Bond Formation
From http://www.piercenet.com/media/Sulfo-NHS_Reaction_Figure03.gif

2.1.1. AuNP Addition

The next stage in probe assembly was the addition of AuNP. These were allowed to bind to the thiol groups on the cysteine residue near the C-terminus of the designed peptide linkers. AuNP was added at the desired molar ratio and allowed to react overnight. Any excess AuNP were then removed by centrifugation via a 50 kDa cutoff centrifugal filter (Amicon).

2.1.1. Protection of QD and AuNP Surface with PEG

In order to increase stability and avoid issues such as nonspecific protein adsorption, both the QD surface and AuNP required the addition of PEG. PEG-amine (PEG-NH_2,1000 Da) was added to the QD PAA surface using the carbodiimide chemistry described earlier at a molar ratio of 500:1 PEG:QD and allowed to react overnight. Excess EDC and PEG-NH_2 were removed by dialysis against MilliQ water using a membrane with mesh size of 10 KDa (8 hr, water changed every 2 hr). The AuNP

surface was then functionalized with PEG-thiol (PEG-SH, 1000 Da). This was added at a molar ratio of 100:1 PEG-SH:AuNP and reacted to the AuNP surface via the thiol group on the end of the PEG chain. Following PEG-SH addition, the QD probe mixture was vortexed and allowed to react overnight in the fridge at 4°C. The resulting probes were then again dialyzed and stored under argon.

2.7. Probe Optimization Study

Having established the technique for probe synthesis, optimization of probe characteristics was undertaken. The ideal probe for assaying protease activity will have the greatest sensitivity to protease activity. This is evidenced through the rate of fluorescence recovery exhibited and the overall ratio of fluorescence increase. To optimize these characteristics, two key variables were investigated: the number of AuNP per QD and the peptide linker length. The molar ratio of AuNP:QD was varied at four levels: 5:1, 10:1, 15:1, and 20:1. This was undertaken by varying the molar ratio of peptide linkers to QD as described in the probe design above. The length of the peptide linker was varied at three levels consisting of 0, 2 and 4 glycine spacers on each side of the protease-sensitive site. As amino acids have an average length of approximately 0.38 nm, this coincides to increasing the peptide linker length by 0, 1.52, and 3.04 nm, respectively.

The first step in characterizing the 12 probe formulations was to determine the level of fluorescence quenching in relation to an unquenched QD. For each group, the fluorescence of 1 ml of 20 nM probe solution was measured using a fluorometer (Fluorolog). Three fluorescent measurements of each group were taken using a 425 $\pm$10 nm excitation filter and 590 $\pm$5 emission filter. These were compared to the fluorescence

of a control group subjected to the same reaction conditions as the probes, but without the addition of AuNP.

To determine the level of fluorescence recovery, a second experiment was undertaken. For each of the 12 groups, 0.5 ml of 40 nM probe solution was added to 0.5 ml containing 0.1 FALGPA units of collagenase from *Clostridium histolyticum* (Sigma) with a specific activity of 0.5 units/mg. An FALGPA unit is defined by the manufacturer as the amount of enzyme required to hydrolyze 1.0 μm of furylacryloyl-LGPA per min at pH 7.5 and 25 °C in the presence of calcium ions. Fluorescence readings were taken of the solution in 1 ml disposable plastic cuvettes using a fluorometer (Fluorolog) at 5 min intervals for the first hour. The QD probes, having a peak excitation of 592 nm, were excited using a 425 ± 10 nm excitation filter and emissions were collected using a 590 ± 5 nm emission filter.

2.7. Multiplexing Study

In order to demonstrate the ability of the probes to be used in multiplexed applications, cathepsin K and collagenase activity were simultaneously monitored in solution. In addition to the collagenase sensitive probes (emission at 592 nm, degradable peptide: GGGGLGPAGGGGC, AuNP:QD ratio of 10:1) used earlier, a new batch of cathepsin K sensitive probes (emission at 541 nm, degradable peptide: GGGMGPSGPWGGC, AuNP:QD ratio of 10:1) was synthesized as previously described.

In the first experiment, 0.5 ml containing 5 pmol of both collagenase and cathepsin K sensitive probes was incubated with 0.5 ml of an enzyme solution containing either collagenase (0.1 FALGPA units), cathepsin K (0.005 units), or both. A cathepsin

K unit is defined by the manufacturer as the amount of enzyme required to hydrolyze 1.0 μm of Phe-Arg per min at pH 7.5 and 25 °C. The solution was excited using a 425 ± 10 nm filter and readings of collagenase probe fluorescence (590 ± 5 nm emission filter) and cathepsin K probe fluorescence (540 ± 10 nm filter) were taken with a fluorometer every 5 min for 1 hr.

Chapter 3: Results

3.1. QD Characterization

3.1.1. TEM Images - Size

The first parameter that needed to be characterized for QD was their size. This was accomplished using TEM imaging. Figure 24 shows such sample images after shelling, after PAA-OA water solubilization, and after AuNP addition. It can be seen that the QD go from about 7-8nm diameter after shelling to about 30 nm after water solubilization.

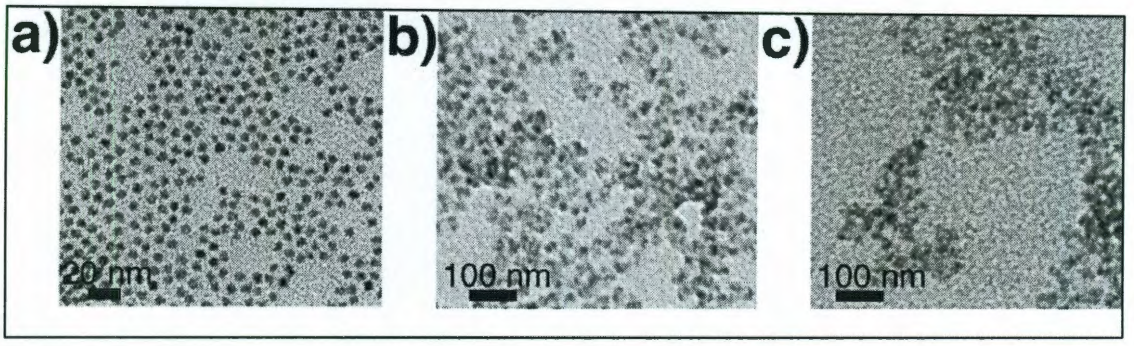

Figure 24 - TEM images at various stages - TEM images of the probes after a) ZnS Shelling, b) water solubilization, and c) addition of AuNP. TEM images were taken at 60000x.

3.1.2. ICP/OES - Concentration

Determining the concentration of QD was the next step and is crucial to ensure repeatability of future studies. After digestion of 100 µL, ICP measurements were taken to get concentrations of Cd in ppm. From this value we can calculate our original stock concentration and then using the following equations and approximations we can get the particle concentration.

$$Length\ of\ CdSe\ Bond = 0.36nm$$

$$\#\ of\ Units\ in\ Diameter = D/0.36$$

$$\#\ of\ CdSe\ in\ Sphere = \frac{4\pi(units)^2}{3}$$

$$Weight\ of\ Cd\ per\ mol\ of\ QD = 114 * \#\ of\ CdSe$$

$$Mol\ of\ Stock\ Sol. = PPM(mg/L)/(Weight\ Cd/mol\ QD)$$

3.1.3. UV-VIS – Absorbance Spectra

Finally, absorbance measurements were taken after core synthesis, shelling, and water solubilization. Both peak absorbance and full width at half maximum were calculated. Figure 25 shows three sample spectra. The top spectrum is that of just CdSe cores. The second spectrum is after 3 Zn/S shells have been added. It can be noted that shelling causes a shift in peak absorption. Finally, the third spectrum is for PAA-OA water solubilized QD. Again there is a shift in peak absorbance although this shift is a small one.

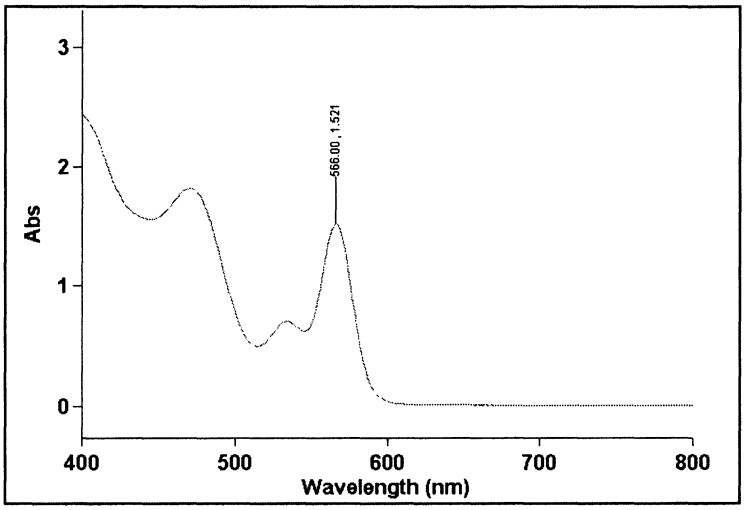

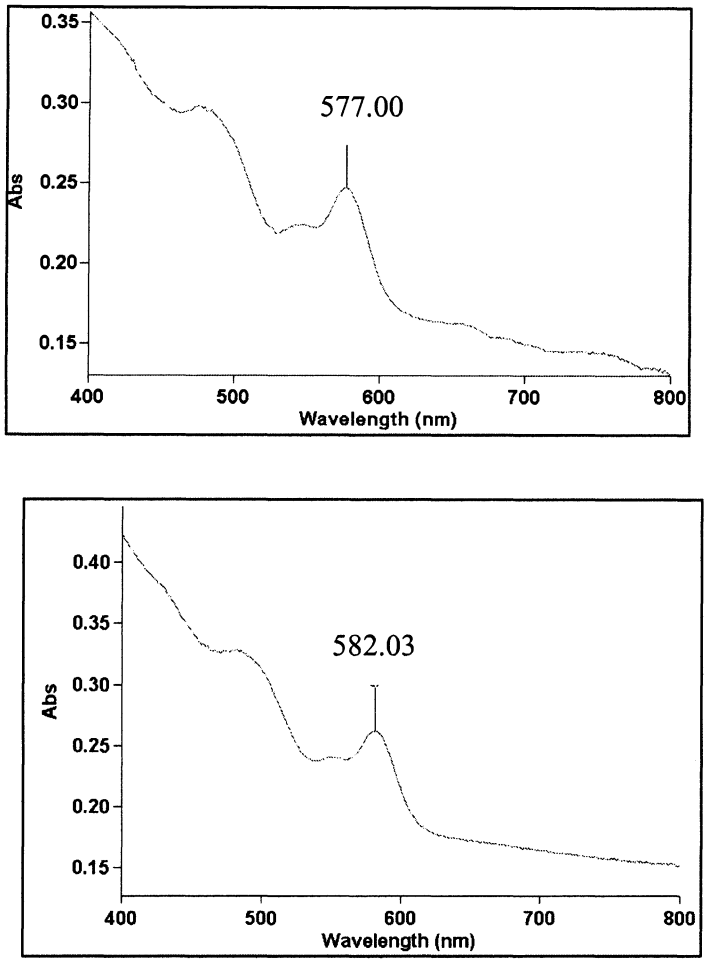

Figure 25 - Absorbance Spectra of CdSe , CdSeZnS, and PAA-OA coated QD

3.2. MALDI-TOF ANALYSIS

The successful synthesis of all peptides synthesized was undertaken using MALDI-TOF analysis. This ensured that the synthesis was completed successfully and that no amino acids were left out during synthesis. As well, a study was carried out in which spectra of the peptide before and after incubation with protease were taken. This was done to ensure that linkers were in fact being cleaved. Figure 22 shows a

representative result for GGLGPAGGC before and after cleavage. Of note is the fact that we see a disappearance in the main peak of the peptide at around 960 Da indicating cleavage is taking place.

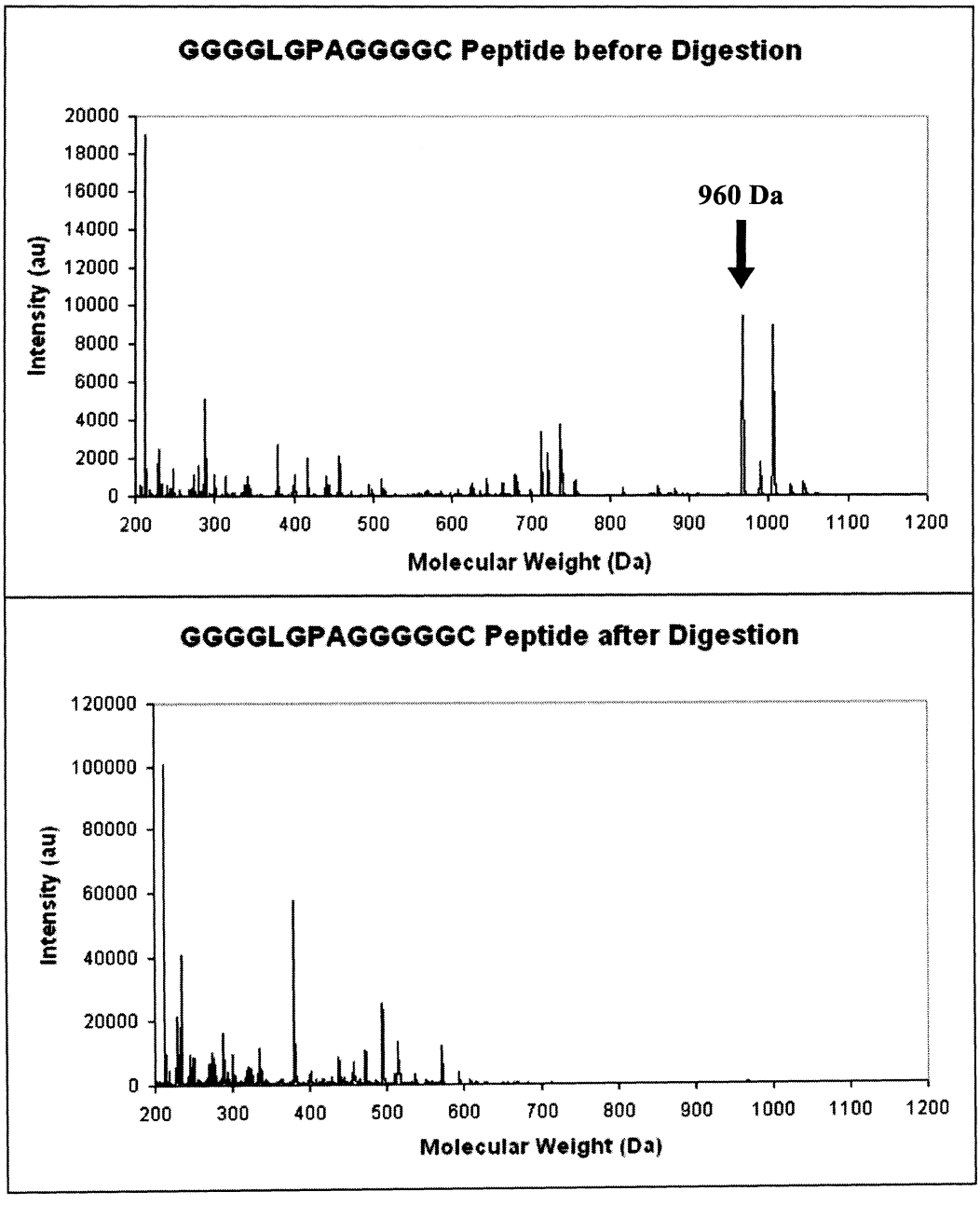

Figure 26 - MALDI-TOF of Peptide Before and After Digestion

3.3. Validation of Probe Functionality

To ensure that probe assembly was successful, a simple study was run in which a batch of probes was incubated with 0.2 mg/ml of collagenase. The emission spectra of the probes before and after incubation as well as a control were taken. In Figure 27, we see the difference between the control (solid line) and probe (dashed). After 1 hr of incubation with collagenase we see a restoration of the emission (dotted line)

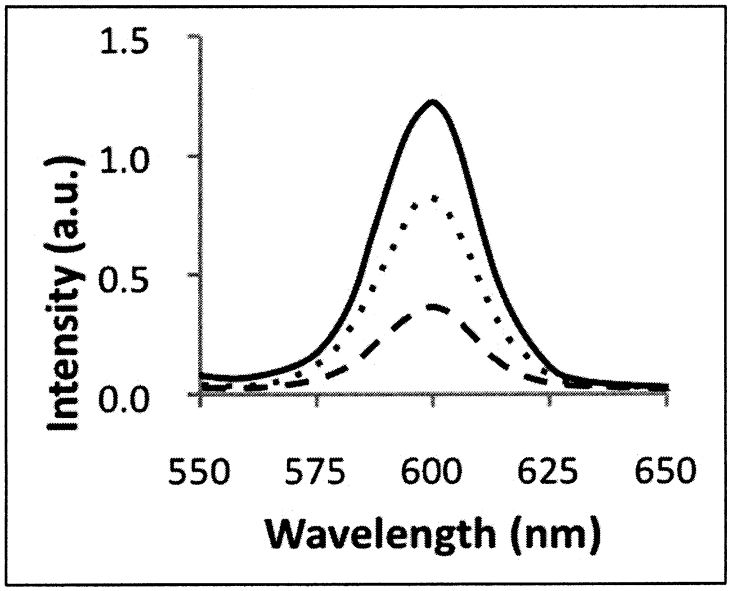

Figure 27 – Validation of Successful Probe - Fluorescence intensity of control (no AuNP, solid line) and quenched QD probes (dashed line), and recovered fluorescence of activated QD probes following incubation with collagenase (dotted line).

3.4. Determination of Probe Quenching

In order to compare the level of quenching produced by the varying linker lengths and AuNP:QD ratios, each group was measured with respect to a control with no AuNP. The results of these fluorescence measurements can be seen in Figure 28.

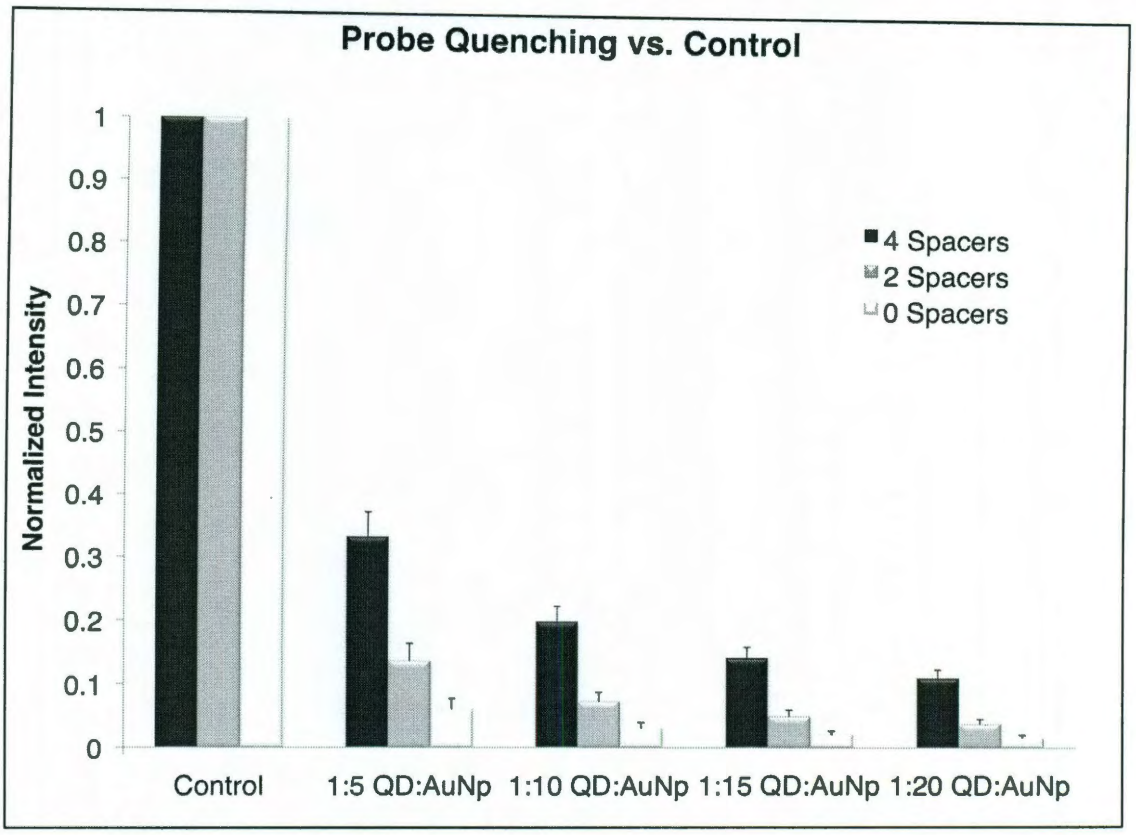

Figure 28 - Degree of Quenching vs. Control - The level of quenching of each of the 12 groups is measured with respect to a control using a fluorometer to determine the level of quenching.

As seen in Figure 28, the magnitude of QD quenching is increased by both decreasing the glycine spacer length and increasing the number of AuNP attached to the probes. These changes were statistically significant for all the levels evaluated (ANOVA, with Tukey's post hoc, $p<0.01$). Based on these results and analysis of the Forster formalism, probes containing spacers of greater than 4 glycines were not investigated as they would likely result in a dramatic decrease in the level of quenching and thus decrease probe performance.

3.5. Optimization of Fluorescence Recovery of Probes

Having determined the varying levels of probe quenching, the next step was to compare the fluorescence recovery of the various probes in the presence of protease. All 12 groups were exposed to a 0.2 mg/ml solution of collagenase and the fluorescence was monitored over the first hour. The results of this study can be seen in Figure 29. Of note is the absence of the probes with 0 length spacers. Probes with 0 glycine spacers had minimal fluorescent recovery, likely due to impaired protease access to the degradation site at such short linker lengths.

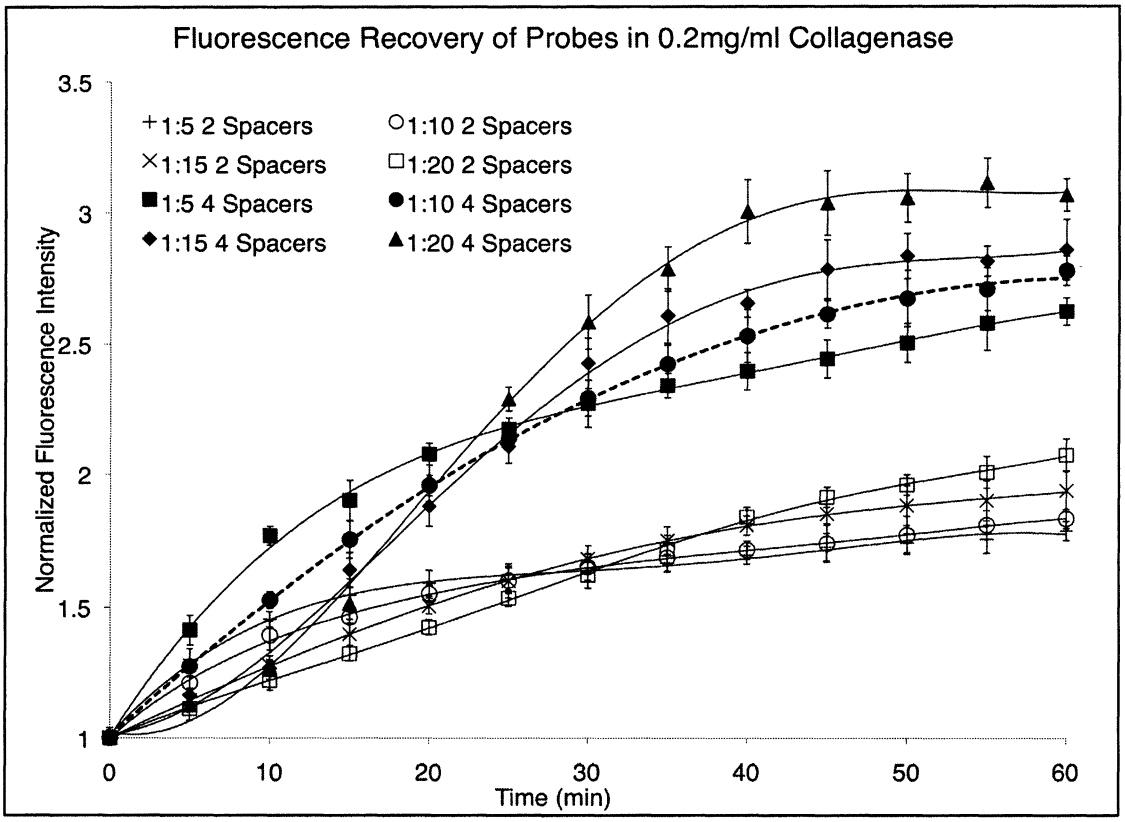

Figure 29 - Fluoresecence Recovery of Probes in the Presence of Collagenase - Probes with 1-10:1 4 spacers (dashed line) were chosen as the best formulation.

The probe formulation demonstrating the most desirable response in the presence of enzyme uses degradable peptide linkers with 4 glycine spacers to join AuNP to QD at a ratio of 10:1 (Figure 3b, filled circles dashed line). These particles have good initial quenching and high overall fluorescence recovery, and also exhibit a fast and linear response in the initial 15 min of activation providing sensitivity as well as ease of quantification.

3.6. Multiplexing Probes Sensitive to Collagenase and Cathepsin K

In order to demonstrate the ability to multiplex probes, a solution containing both collagenase and cathepsin K probes was incubated with either or both of the proteases. As demonstrated in Figure 30, the addition of a single enzyme results in activation of a single QD probe (panels a and b) with only low levels of cross-activation of the non-specific QD. The specific activation of two QD probes at similar levels of intensity was accomplished upon exposure to the dual enzyme solution (Figure 30, c). The ability of QD to specifically recognize individual proteases with good signal to noise means that using this technology in multiplexed applications is quite feasible.

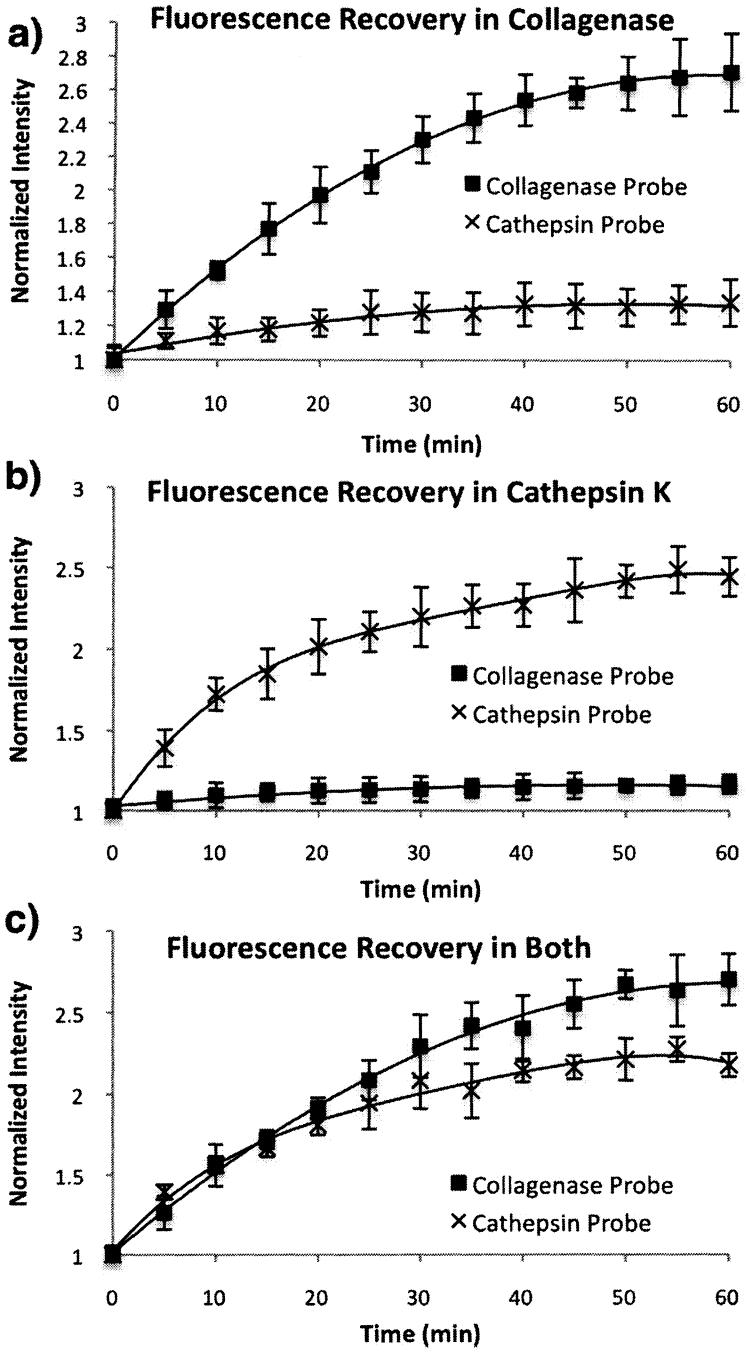

Figure 30 – Multiplexing Proof of Concept - Fluorescent signal gain of both collagenase and cathepsin K sensitive probes when incubated with a) 0.1 units of collagenase b) 0.005 units of cathepsin K c) 0.1 units of collagenase and 0.005 units of cathepsin K.

Chapter 4: Discussion

This work has demonstrated the ability to produce protease-activated quantum dot probes. Initially, a proof of concept study was carried out which validated the probe assembly technique. It was found that it is important to first attach the linkers, then the AuNP, and finally to backfill with PEG. If the QD surface is first protected with PEG, attachment of the linker and AuNP become much more difficult.

Having validated general functionality, a study was designed to optimize probe functionality. In order to better analyze the levels of quenching of the 12 groups and gain insight into probe conformation, the data was fit to the Forster formalism:

$$E = \frac{n}{n + \left(\frac{r}{R_0}\right)^6}$$

In this equation, E represents the FRET or shielding efficiency (% of fluorescence shielded), n is the number of AuNP quenchers per QD, r is the separation of the QD and AuNP, and R_0 is the Forster radius. Previous work by Gueroui *et al.*[138] has shown the R_o for AuNP/QD quenching to be 7.5 nm. Solving for r at the 0, 2 and 4 spacer linker lengths yields separations of 2.97, 2.48, and 1.63 nm. As linker length is increased, the ratio of spacing/linker length decreases, indicating the AuNP are bending more towards the QD.

The study carried out to optimize probe functionality showed that probes with 4 spacers and AuNP:QD ratio of 10:1 produced the best results. This validated the theory that there is a distinct interplay between the effects of steric hindrance/ cleavage site accessibility and overall probe quenching. Further, when examining the recovery in

fluorescence of the probes, it is seen that this recovery can be modeled as a logistic function. As the enzymes cleave AuNP from the QD, steric hindrance is reduced and fluorescence recovery accelerates before reaching steady state and leveling off. This effect is more evident in the groups with higher molar ratios of AuNP:QD. This again highlights the complex interactions and competing factors that are involved in this probe design.

Finally, a study was undertaken to demonstrate the multiplexing ability of these protease-activated QD probes. The ease of designing peptide linkers specific to any protease of choice was demonstrated. By scanning literature and/or using tools such as the MEROPS peptidase database, one could easily select several key sequences pertaining to the proteases one wishes to study. Each of a series of batches of QD of various sizes (and thus with orthogonal emission spectra) could then be used to assemble probes with a protease target of choice. A cocktail of these would be able to monitor several proteases concurrently in addition to enabling quantification of the data.

Chapter 4: Conclusions

Protease-Activated quantum dot probes have been synthesized and it has been shown that their fluorescence change correlates with protease activity. Having validated general synthesis strategy, a study was carried out which allowed probe configuration to be optimized.

The effect of linker length and AuNP:QD ratio on fluorescence recovery were explored and it was shown that probes with 4 spacers and 10:1 AuNP:QD ratio produced optimal results. This was the configuration at which the steric hindrance caused by shorter linkers and more AuNP balanced with the gain in potential fluorescent recovery. To further demonstrate the potential applications of these probes, it was shown that multiple probes each sensitive to a specific protease can simultaneously be used to monitor protease activity.

This work has laid the foundation for protease-activated quantum dot probes. Further work needs to be carried out to demonstrate the functionality of the probes in a complex biological environment. This work can be carried out using cell lines such as NIH-3T3, HT1080, and MCF-7 with varying degrees of metastatic potential. Upon demonstration of functionality *in vitro,* an *in vivo* model using immuno-compromised Balb/c nude mice model should be used to validate the probes ability to quantify protease expression in various tumor types.

References

[1] Myer J. and Ginsburg G. (2002). The path to personalized medicine. *Current Opinion in Chemical Biology.* 6:434–438.

[2] Agrawal S. and Khan F. (2007). Human Genetic Variation and Personalized Medicine. *Indian J Physiol Pharmacol.* 51(1) : 7–28

[3]Redd WH, Montgomery GH, and DuHamel KN. (2001). Behavioral intervention for cancer treatment side effects. *J Natl Cancer Inst.* 93(11):810-23.

[4] Herbst, R.S. et al. (2005). Clinical cancer advances 2005: major research advances in cancer treatment, prevention, and screening—a report from the American Society of Clinical Oncology. *J. Clin. Oncol.* 24: 190–205.

[5] Potti et.al. (2006). Genomic Signatures to Guide the Use of Chemotherapeutics. *Nature Medicine.* 12: 1294.

[6] Ludwig JA, and Weinstein JN. (2005) Biomarkers in cancer staging, prognosis and treatment selection. *Nature Reviews in Cancer. 5(11):845-56.*

[7] Kos J, Lah TT. (1998). Cysteine proteinases and their endogenous inhibitors: target proteins for prognosis, diagnosis and therapy in cancer (review). *Oncol Rep.* (6):1349-61.

[8] Bridges SL Jr. (1999). The genetics of rheumatoid arthritis: Influences susceptibility, severity, and treatment response. *Curr Rheumatol Rep.* 1(2):164-71.

[9] Weinshilboum R. (2003). Inheritance and drug response. *New England Journal of Medicine.* 348: 529–537.

[10] Eichelbaum M, Ingelman-Sundberg M, Evans WE. (2006). Pharmacogenomics and individualized drug therapy. *Annu Rev Med.* 57:119-37.

[11] Meyer UA. (2004. *Nat Rev Genetics.* 5(9): 669 – 676.

[12] Vogel, F. (1959). Moderne Probleme der Humangenetik. Ergebn. *Inn. Med. Kinderheilkd.* 12: 52–125.

[13] International Human Genome Sequencing Consortium (2001). Initial sequencing and analysis of the human genome.. *Nature* 409: 860–921.

[14] Janne, P. A. et al. (2004) High-resolution single-nucleotide polymorphism array and clustering analysis of loss of heterozygosity in human lung cancer cell lines. *Oncogene.* 23: 2716–2726.

---

[15] Veer L.J. and Bernards R. (2008). Enabling personalized cancer medicine through analysis of gene-expression patterns. 452(3): 564-570.

[16] Pellet, C. et al. (2001). Virologic and immunologic parameters that predict clinical response of AIDS-associated Kaposi's sarcoma to highly active antiretroviral therapy. *J. Invest. Dermatol.* 117: 858–863.

[17] Bianchi, N. O., Bianchi, M. S. & Richard, S. M. (2001). Mitochondrial genome instability in human cancers. *Mutat. Res.* 488: 9–23.

[18] Omenn, G. S. (2004). Advancement of biomarker discovery and validation through the HUPO plasma proteome project. *Dis. Markers.* 20: 131-134.

[19] Ma Y, Ding Z, Qian Y, Shi X, Castranova V, Harner EJ, Guo L. (2006). Predicting cancer drug response by proteomic profiling. *Clin Cancer Res.* 12(15):4583-9.

[20] Petricoin E., Paweletz C., and Liotta L. (2002). Clinical Applications of Proteomics: Proteomic Pattern Diagnostics. *Journal of Mammary Gland Biology and Neoplasia,* 4:433-440.

[21] Duffy M. (1996). Protaeases as Prognostic Markers in Cancer. *Clincial Cancer Research.* 2: 613-618.

[22] Decock J, Paridaens R, Cufer T. (2005). Proteases and metastasis: clinical relevance nowadays? *Curr Opin Oncol.* 17(6):545-50.

[23] Hooper, N. M. (2002). *Proteases in Biology and Medicine.* London: Portland Press.

[24] Barrett, A. J., Rawlings, N. D. & Woessner, J. F. (1998) *Handbook of Proteolytic Enzymes.* San Diego: Academic Press.

[25] Puente, X. S., Sanchez, L. M., Overall, C. M. & Lopez-Otin, C. (2003). Human and mouse proteases: A comparative genomic approach. *Nature Reviews Genetics.* 4, 544–558.

[26] Overall C. and Blobel C. (2007). In search of partners: linking extracellular proteases to substrates. *Nature Reviews.* 3: 185-194.

[27] Egeblad, M. & Werb, Z. (2002) New functions for the matrix metalloproteinases in cancer progression. *Nature Reviews in Cancer.* 2: 161–174.

[28] Liotta LA, Tryggvason K, Garbisa S, Hart I, Foltz CM, and Shafie S. (1980).Metastatic potential correlates with enzymatic degradation of base- ment membrane collagen. *Nature.* 284: 67–68.

[29] Hanahan, D. and Weinberg, R. (2000). The hallmarks of cancer. *Cell.* 100: 57–70.

---

[30] Egelbad M. and Werb Z. (2002). New functions for the matrix metalloproteinases in cancer progression. *Nature Reviews Cancer.* 2: 161-174.

[31] Peschon, J. J. et al. (1998). An essential role for ectodomain shedding in mammalian development. *Science.* 282: 1281–1284.

[32] Manes, S. et al. (1999). The matrix metalloproteinase-9 regulates the insulin-like growth factor-triggered autocrine response in DU-145 carcinoma cells. *J. Biol. Chem.* 274: 6935–6945.

[33] Agrez, M., Chen, A., Cone, R. I., Pytela, R. and Sheppard, D. (1994). The αvβ6 integrin promotes proliferation of colon carcinoma cells through a unique region of the β6 cytoplasmic domain. *J. Cell Biol.* 127: 547–556.

[34] Reed J. (1999). Mechanisms of apoptosis avoidance in Cancer. *Cancer Biology.* 11: 68-75.

[35] Sheu, B.-C. et al. (2001). A novel role of metalloproteinase in cancer-mediated immunosuppression. *Cancer Res.* 61:237–242.

[36] Gorelik, L. & Flavell, R. A. (2001). Immune-mediated eradication of tumors through the blockade of transforming growth factor-β signaling in T cells. *Nature Med.* 7: 1118–1122.

[37] Kataoka, H. et al. (1999). Enhanced tumor growth and invasiveness in vivo by a carboxyl-terminal fragment of α1-proteinase inhibitor generated by matrix metalloproteinases: a possible modulatory role in natural killer cytotoxicity. *Am. J. Pathol.* 154: 457–468.

[38] Xu, J. et al. (2001). Proteolytic exposure of a cryptic site within collagen type IV is required for angiogenesis and tumor growth in vivo. *J. Cell Biol.* 154: 1069–1080.

[39] Bergers, G. et al. (2002). Matrix metalloproteinase-9 triggers the angiogenic switch during carcinogenesis. *Nature Cell Biol* .2: 737–744.

[40] Hiraoka, N., Allen, E., Apel, I., Gyetko, M., and Weiss, S. (1998). Matrix metalloproteinases regulate neovascularization by acting as pericellular fibrinolysins. *Cell.* 95: 365–377.

[41] Ossowski, L., Clunie, G., Masucci, M.T., and Blasi, F. (1991). In vivo paracrine interaction between urokinase and its receptor: Effect on tumor cell invasion. *J. Cell Biol.* 115: 1107–1112.

[42] Sloane BF, Dunn JR, and Honn KV. (1981). Lysosomal cathepsin B: correlation with metastatic potential. *Science.* 212: 1151-3.

[43] Giannelli, G., Falk-Marzillier, J., Schiraldi, O., Stetler-Stevenson, W. G., and Quaranta, V. (1997). Induction of cell migration by matrix metalloprotease-2 cleavage of laminin-5. *Science.* 277: 225–228.

[44] Kajita, M. et al. (2001). Membrane-type 1 matrix metalloproteinase cleaves CD44 and promotes cell migration. *J. Cell Biol.* 153: 893–904.

[45] Birchmeier, C., Birchmeier, W. and Brand-Saberi, B. (1996). Epithelial–mesenchymal transitions in cancer progression. *Acta Anat. (Basel.).* 156: 217–226.

[46] Kim, J., Yu, W., Kovalski, K., and Ossowski, L. (1998). Requirement for specific proteases in cancer cell intravasation as revealed by a novel semiquantitative PCR-based assay. *Cell.* 94: 353–362

[47] Sternlicht, M.D. and Werb, Z. (2001). How matrix metalloproteinases regulate cell behavior. *Annu. Rev. Cell Dev. Biol.*17: 463–516.

[48] Scarisbrick, I. A. (2008). The Multiple Sclerosis Degradome: Enzymatic Cascades in Development and Progression of Central Nervous System Inflammatory Disease. In M. Rodriguez, pAdvances in Multiple Sclerosisand Experimental Demyelinating Diseases. Current Topics in Microbiology and Immunology (pp. 133-175). Heidelberg : Springer-Verlag Berlin .

[49] Mastroianni, C.M. and Liuzzi G.M. (2007) Matrix metalloproteinase dysregulation in HIV infection: implications for therapeutic strategies. *Trends in Molecular Medicine.* 11:449-59.

[50] Reed, C. and Kita, H. (2004) The role of protease activation of inflammation in allergic respiratory diseases. *J Allergy Clin Immunol* 114:997-1008.

[51] Richard, I. (2005). The genetic and molecular bases of monogenic disorders affecting proteolytic systems. *Journal Medical Genet*ics 42: 529–539.

[52] Turk B. (2006). Targeting Proteases: Successes, Failures, and Future Prospects. *Nature Reviews in Drug Discovery.* 5: 785-799.

[53] Luciani F. , Kesxmir C., Mishto M., Or-Guil M., and Boery R. (2005). A Mathematical Model of Protein Degradation by the Proteasome. *Biophysical Journal.* 88: 2422–2432.

[54] Stachowiak K., Tokmina M., Karpińska A., Sosnowska R., and Wiczk W. (2004). Fluorogenic peptide substrates for carboxydipeptidase activity of cathepsin B. *Acta Biochimica Polonica.* 51: 81-92.

[55] Ayalya Y. and Di Cera E. (2000) A simple method for the determination of individual rate constants for substrate hydrolysis by serine proteases. *Protein Science.* 9:1589-1593.

---

[56] Schulz O., Sewell H.F., and Shakib F. (1998). A sensitive fluorescent assay for measuring the cysteine protease activity of Der p 1, a major allergen from the dust mite Der matophagoides pteronyssinus. *J Clin Pathol: Mol Pathol.* 51:222–231.

[57] Michaelis and Menten (1913). Biochem. Z. 49, 333.

[58] Ratkowsky D.A. (1986) A suitable parameterization of the Michaelis-Menten enzyme reaction. Biochem. J. 240: 357-360.

[59] Schwartz, D.R. et al. (2007). Hu/Mu ProtIn oligonucleotide microarray: dual-species array for profiling protease and protease inhibitor gene expression in tumors and their microenvironment. *Mol. Cancer Res.* 5: 443–454.

[60] Overall, C.M., et al. (2004). Protease degradomics: mass spectrometry discovery of protease substrates and the CLIP-CHIP, a dedicated DNA microarray of all human proteases and inhibitors. *Biol. Chem.* 6: 493–504.

[61] Riddick, A.C. et al. (2005). Identification of degradome components associated with prostate cancer progression by expression analysis of human prostatic tissues. *British Journal of Cancer.* 12: 2171–2180.

[62] Aebersold, R. and Mann, M., (2003). Mass spectrometry-based proteomics. *Nature* 422: 198–207.

[63] Link, A.J., et al. (1999). Direct analysis of protein complexes using mass spectrometry. *Nat. Biotechnol.* 7: 676–682.

[64] Creasy B., Hartmann C., White F., an Mccoy K. (2007). New Assay Using Fluorogenic Substrates and Immunofluorescence Staining to Measure Cysteine Cathepsin Activity in Live Cell Subpopulations. *Cytometry Part A.* 2: 114-123.

[65] Zhang Z., Yan J., Lu J., Lin J., Zeng S., an Luo Q. (2008). Fluorescence imaging to assess the matrix metalloproteinase activity and its inhibitor in vivo. *Journal of Biomedical Optics.* 13(1): 01106-1-6.

[66] Martin S., Hattersley N., Samule I., Hay R., and Tatham M. (2007). A Fluorescence-resonance-energy-transfer-based protease activity assay and its use to monitor paralog-specific small ubiquitin-like modifier processing. *Analytical Biochemistry.* 363:83-90.

[67] Förster T. (1948) Zwischenmolekulare Energiewanderung und Fluoreszenz, *Ann. Physik.* 437: 55

[68] Rudolf et al. (2003). Looking Forward to Seeing Calcium. *Nature Reviews in Molecular Cell Biology.* 7: 579.

---

[69] Sieber, S.A., Niessen, S., Hoover, H.S. & Cravatt, B.F. (2006). Proteomic profiling of metallo-protease activities with cocktails of active-site probes. *Nat. Chem. Biol.* 2: 274–281.

[70] Kato, D. et al. (2005). Activity-based probes that target diverse cysteine protease families. *Nat. Chem. Biol.* 1: 33–38.

[71] Saghatelian, A., Jessani, N., Joseph, A., Humphrey, M. & Cravatt, B.F. (2004). Activity-based probes for the proteomic profiling of metalloproteases. *Proc. Natl. Acad. Sci. USA.* 101: 10000–10005.

[72] Blum G. , Mullins S., Keren K., Fonovic M., Jeeszko C., Rice M., Sloane B., and Bogyo M. (2005). Dynamic imaging of protease activity with fluorescently quenched activity-based probes. *Nature Chemical Biology.* 4: 203-209.

[73] M.S. Stack, and R.D. Gray. (1989). Comparison of vertebrate collagenase and gelatinase using a new fluorogenic substrate peptide. *J. Biol. Chem.* 264: 4277–4281

[74] C.G. Knight, F. Willenbrock, G. Murphy. (1992). A novel coumarin-labelled peptide for sensitive continuous assays of matrix metalloproteinase's. *FEBS Lett.* 296 263–266.

[75] E.D. Matayoshi, G.T. Wang, G.A. Krafft, and J. Erickson. (1990). Novel fluoro-genic substrates for assaying retroviral proteases by resonance energy transfer. *Science* 247: 954–958.

[76] J. Peppard, Q. Pham, A. Clark, D. Farley, Y. Sakane, R. Graves, et al. (2003). Development of an assay suitable for high-throughput screening to measure matrix metalloprotease activity. *Assay Drug Dev. Technol.* 1: 425–433.

[77] Salisbury CM, Maly DJ, and Ellman JA. (2002). Peptide microarrays for the determination of protease substrate specificity. *J Am Chem Soc.* 124: 14868-70.

[78] Mahmood, U., Tung, C., Bogdanov, A., and Weissleder, R. (1999). Near infrared optical imaging system to detect tumor protease activity. *Radiology.* 213: 866 – 870.

[79] Tung, C., Mahmood, U., Bredow S., and Weissleder, R. (2000). In Vivo Imaging of Proteolytic Enzyme Activity Using a Novel Molecular Reporter. *Cancer Research.* 6:, 4953– 4958.

[80] Chen J. et al. (2005). Near-Infrared Fluorescent Imaging of Matrix Metalloproteinase Activity After Myocardial Infarction. *Circulation.* 111:1800-1805.

[81] Lakowicz, J. R. (1999). Principles of Fluorescence Spectroscopy 2nd edn. Kluwer Academic/Plenum.

[82] Zhang, J., Campbell, R. E., Ting, A. Y. and Tsien, R. Y. (2002). Creating new fluorescent probes for cell biology. *Nature Rev. Mol. Cell Biol.* 3: 906–918.

---

[83] Chan, W.C.W. et al. (2002) Luminescent QDs for multiplexed biological detection and imaging. *Current Opinions in Biotechnology*. 13: 40–46 .

[84] Akerman, M.E., Chan, W.C.W., Laakkonen, P., Bhatia, S.N. & Ruoslahti, E. (2002).

Nanocrystal targeting in vivo. Proc. Natl. Acad. Sci. USA. 99: 12617–12621.

[85] Wu, X.Y. et al. (2003). Immunofluorescent labeling of cancer marker Her2 and other cellular targets with semiconductor QDs. *Nature Biotechnology*. 21: 41–46.

[86] Nathaniel G. Portney . Mihrimah Ozkan. (2006) Nano-oncology: drug delivery, imaging, and sensing. *Anal Bioanal Chem* 384: 620–630

[87] Alivisatos P., Gu W., and Larabell C. (2005). Quantum Dots as Cellular Probes. *Annual Reviews in Biomedical Engineering* 7:55-76.

[88] Hines MA, Guyot-Sionnest P. (1996). Synthesis and characterization of strongly

luminescing ZnS-capped CdSe nanocrystals. *J. Phys. Chem.* 100:468–71

[89] Michalet X, Pinaud FF, Bentolila LA, Tsay JM, Doose S, Li JJ, Sundaresan G, Wu AM, Gambhir SS, Weiss S. (2005) Quantum Dots for Live Cells, in Vivo Imaging, and Diagnostics. *Science*. 307: 538-44.

[90] Igor L. Medintz, H. Tetsuo Uyeda, Ellen R. Goldman and Hedi Mattoussi. (2005). Quantum dot bioconjugates for imaging, labelling and sensing. *Nature Materials*. 4: 435 - 446

[91] Michalet X, Pinaud F, Lacoste TD, Dahan, M, Bruchez M, et al. (2001). Properties of

fluorescent semiconductor nanocrystals and their applications to biological labeling. *Single Mol.* 2:261–76.

[92] Bruchez M, Moronne M, Gin P, Weiss S, Alivisatos AP. (1998). Semiconductor

nanocrystals as fluorescent biological labels. *Science* 281:2013–16.

[93] Xiaohu Gao, Yuanyuan Cui, Richard M Levenson, Leland W K Chung and Shuming Niel. (2004). *In vivo* cancer targeting and imaging with semiconductor quantum dots. *Nature Biotechnology*. 8: 969-76.

[94] Jaiswal JK, Mattoussi H, Mauro JM, Simon SM. (2003). Long-term multiple color imaging of live cells using quantum dot bioconjugates. *Nat Biotechnol*. 21: 47-51.

[95] Larson D.R. (2003). Water-soluble quantum dots for multiphoton fluorescence imaging in vivo. *Science*. 300: 1434-1436.

---

[96] Gao et al. (2004). *In vivo* cancer targeting and imaging with semiconductor quantum dots. *Nature Biotechnology.* 8: 969-976.

[97] Weissleder R. (2001). A clearer vision for *in vivo* imaging. *Nat. Biotech.* 19: 316-7.

[98] Willard, D. M., Carillo, L. L., Jung, J. & Van Orden, (2001) A. CdSe-ZnS quantum dots as resonance energy transfer donors in a model protein-protein binding assay. *Nano Letters.* 1: 469–474.

[99] Chan WCW, Nie S (1998). Nanocrystal targeting in vivo. *Science* 281: 2016–2018

[100] Uyeda HT, Medintz IL, Jaiswal JK, Simon SM, Mattoussi H. (2005). Quantum dot bioconjugates for imaging, labelling and sensing. *Journal American Chemical Society.* 127:3870-3878.

[101] Mattoussi, H. et al. (2000). Self-assembly of CdSe-ZnS quantum dot bioconjugates using an engineered recombinant protein. *Journal American Chemical Society.* 122: 12142–12150.

[102] Gerion, D. et al. (2001). Synthesis and properties of biocompatible water-soluble silica coated CdSe/ZnS semiconductor quantum dots. *Journal of Physical Chmistry.* 105:

8861–8871.

[103] Darbandi M, Thomann R, Nann T (2005) Single quantum dots in silica spheres by microemulsion synthesis. *Chem Mater.* 17: 5720

[104] Gao, X., Cui, Y., Levenson, R. M., Chung, L. W. K. & Nie, S. (2004). In vivo cancer targeting and imaging with semiconductor quantum dots. *Nature Biotechnology.* 22: 969–976.

[105] T. Pellegrino, L. Manna, S. Kudera, T. Liedl, D. Koktysh, A.L. Rogach, S. Keller, J. Raedler, G. Natile, W.J. Parak. (2004) Hydrophobic nanocrystals coated with an amphiphilic polymer shell: a general route to water soluble nanocrystals. *Nano Letters* 4: 703–707.

[106] Osaki, F., Kanamori, T., Sando, S., Sera, T. & Aoyama, Y. (2004). A quantum dot conjugated sugar ball and its cellular uptake on the size effects of endocytosis in the subviral region. *Journal of the American Chemical Society.* 126: 6520–6521.

[107] Dubertret, B. et al. (2002). In vivo imaging of quantum dots encapsulated in

phospholipids micelles. *Science.* 298: 1759–1762.

[108] Lidke et al. (2004). Quantum dot ligands provide new insights into erbB/HER receptor-mediated signal transduction. *Nat. Biotechnol.* 22: 198–203.

[109] Dahan M. et al. (2003). Diffusion dynamics of glycine receptors revealed by single-quantum dot tracking, *Science.* 302: 442–445.

[110] Lieleg O. et al. (2007). Specific integrin labeling in living celts using functionalized nanocrystals. *Small.* 3: 1560–1565.

[111] Jaiswal J.K., Goldman E.R., Mattoussi H., and Simon S.M. (2004). Use of quantum dots for live cell imaging. *Nat. Methods.* 1:73–78.

[112] Hanaki K. et al. (2003). Semiconductor quantum dot/albumin complex is a long-life and highly photostable endosome marker. *Biochem. Biophys. Res. Commun.* 302: 496-501.

[113] Delehanty J.B et al. (2006). Self-assembled quantum dot–peptide bioconjugates for selective intracellular delivery, *Bioconjug. Chem.* 17: 920–927.

[114] Derfus A.M, Chan W., and Bhatia S.N. (2004). Intracellular delivery of quantum dots for live cell labeling and organelle tracking, *Adv. Mater.* 16: 961–966.

[115] Chen F. and Gerion D. (2004). Fluorescent CdSe/ZnS nanocrystal–peptide conjugates for long-term, nontoxic imaging and nuclear targeting in living cells. *Nano Lett.* 4: 1827–1832.

[116] Conner S. and Schmid, S. (2003). Regulated portals of entry into the cell. *Nature.* 422: 37–44.

[117] Ruan G., Agrawal A, Marcus A, and Nie S. (2007). Imaging and tracking of Tat peptide- conjugated quantum dots in living cells: new insights into nanoparticle uptake, intracellular transport, and vesicle shedding, *J. Am. Chem. Soc.* 129: 14759-14766.

[118] Duan H.W. and Nie S.M. (2007). Cell-penetrating quantum dots based on multivalent and endosome-disrupting surface coatings. *J. Am. Chem. Soc.* 129: 3333-3338.

[119] Dubertret B. et al. (2002). In vivo imaging of quantum dots encapsulated in phospholipid micelles. *Science.* 298:1759-1762.

[120] Ballou B, Lagerholm BC, Ernst LA, Bruchez MP, and Waggoner AS. (2004). Noninvasive imaging of quantum dots in mice. *Bioconjug Chem.* 15: 79-86.

[121] Voura EB, Jaiswal JK, Mattoussi H, and Simon SM. (2004). Tracking metastatic tumor cell extravasation with quantum dot nanocrystals and fluorescence emission-scanning microscopy. *Nat. Med.* 10: 993-998.

[122] Zhou M. and Ghosh I. (2006). Current Trends in Peptide Science: Quantum Dots and Peptides: A Bright Future Together. *Peptide Science.* 3: 325-339.

[123] Shi L., Rosenzweig N., and Rosenzweig Z. (2007). Luminescent Quantum Dots Fluorescence Resonance Energy Transfer-Based Probes for Enzymatic Activity and Enzyme Inhibitors. *Anal. Chem.* 79: 208-214.

[124] Shi L., De Paoli V., Rosenzweig N., and Rosenzweig Z. (2006). Synthesis and Application of Quantum Dots FRET-Based Protease Sensors. *Journal of the American Chemical Society.* 128: 10378-379.

[125] Suzuki M., Husimi Y., Komatsu H., Suzuki K., and Douglas K. (2008). Quantum Dot FRET Biosensors that Respond to pH, to Proteolytic or Nucleolytic Cleavage, to DNA Synthesis, or to a Multiplexing Combination. *Journal of the American Chemical Society.* 130: 5720-5725.

[126] Medintz I. et al. (2006). Proteolytic activity monitored by fluorescence resonance energy transfer through quantum-dot–peptide conjugates. *Nature Materials.* 5: 581-589

[127] E. Dulkeith, et al. (2002). Fluorescence quenching of dye molecules near gold nanoparticles: radiative and nonradiative effects. *Phys. Rev. Lett.* 89: 203002.

[128] Z. Gueroui, A. Libchaber. (2004). Single-molecule measurements of gold-quenched quantum dots. *Phys. Rev. Lett.* 9: 166108.

[129] Chang E., Miller J., Sun J., Yu W., Colvin V., Drezek R., and West J. (2005). Proease-activated quantum dot probes. *Biochemical and Biophysical Research Communications.* 334: 1317–1321.

[130] Kim Y., Oh Y., Oh E., Ko S., Han M., and Kim H. (2008). Energy Transfer-Based Multiplexed Assay of Proteases by Using Gold Nanoparticle and Quantum Dot Conjugates on a Surface. *Anal. Chem.* 80: 4634–4641.

[131] Li J. et Al. (2003). Large-Scale Synthesis of Nearly Monodisperse CdSe/CdS Core/Shell Nanocrystals Using Air-Stable Reagents via Successive Ion Layer Adsorption and Reaction. *Journal of the American Chemical Society.* 125: 12567-12575.

[132] Yu W., Qu L., Guo W., and Peng X. (2003). Experimental Determination of the Extinction Coefficient of CdTe, CdSe, and CdS Nanocrystals. *Chem. Mater.* 15: 2854-2860.

[133] Li J.J. et al. (2003). Large-Scale Synthesis of Nearly Monodisperse CdSe/CdS Core/Shell Nanocrystals Using Air-Stable Reagents via Successive Ion Layer Adsorption and Reaction. *Journal of the American Chemical Society.* 125: 12567-12575.

[134] Duff D.G. and Baiker A. (1993). A new hydrosol of gold clusters. *Langmuir.* 9: 2301-2309.

[135] Marokhazi et al. (2004). Enzymic characterization with progress curve analysis of a

collagen peptidase from an enthomopathogenic bacterium, Photorhabdusluminescens. *Biochemistry Journal.* 379: 633-640.

[136] Marokhazi et al. (2004). Enzymic characterization with progress curve analysis of a collagen peptidase from an enthomopathogenic bacterium, Photorhabdusluminescens. *Biochemistry Journal.* 379: 633-640.

[137] West J. and Hubbell J. (1999). Polymeric biomaterials with degradation sites for proteases involved in cell migration. *Macromolecules.* 32: 241–244.

[138] Gueroui Z. and Libchaber A. (2004). Single-molecule measurements of gold-quenched quantum dots. *Physical Review Lett*ers. 9: 166108.